Transverse Chromatic Aberration and Vision: Quantification and Impact across the Visual Field

SIMON WINTER

Doctoral Thesis
Department of Applied Physics
KTH Royal Institute of Technology
Stockholm, Sweden, 2016

TRITA-FYS 2016:19
ISSN 0280-316X
ISRN KTH/FYS/--16:19-SE
ISBN 978-91-7595-980-1

KTH
SE-100 44 Stockholm
SWEDEN

Akademisk avhandling som med tillstånd av Kungliga Tekniska Högskolan framlägges till offentlig granskning för avläggande av teknologie doktorsexamen i fysik fredagen den 3 juni 2016 klockan 10:00 i FD5, AlbaNova Universitetscentrum, Roslagstullsbacken 21, Stockholm.

Print: Universitetsservice US AB
Frontpage: Photograph *Trapped in a prism* by Kit Perren. Printed with permission.

Abstract

The eye is our window to the world. Human vision has therefore been extensively studied over the years. However, in-depth studies are often either limited to our central visual field, or, when extended to the periphery, only correct optical errors related to a narrow spectrum of light. This thesis extends the current knowledge by considering the full visible spectrum over a wide visual field. A broad spectrum means that the wavelength dependence of light propagation inside the eye has to be considered; the optics of the eye will therefore not form a retinal image in the same location for all wavelengths, a phenomenon called chromatic aberration.

We present here a new methodology to objectively measure the magnitude of transverse chromatic aberration (TCA) across the visual field of the human eye, and show that the ocular TCA increases linearly with off-axis angle (about 0.21 arcmin per degree for the spectral range from 543 nm to 842 nm). Moreover, we have implemented adaptive psychophysical methods to quantify the impact of TCA on central and peripheral vision. We have found that inducing additional TCA degrades peripheral grating detection acuity more than foveal resolution acuity (more than 0.05 logMAR per arcmin of induced TCA peripherally compared to 0.03 logMAR/arcmin foveally). As stimuli to evaluate peripheral vision, we recommend gratings that are obliquely-oriented relative to the visual field meridian.

The results of this thesis have clinical relevance for improving peripheral vision and are equally important for retinal imaging techniques. To limit the negative impacts of TCA on vision, inducing additional TCA should be avoided when the peripheral refractive errors are to be corrected, such as for people suffering from macular degeneration and central visual field loss. In retinal imaging applications, TCA leads to lateral offsets when imaging is performed in more than one wavelength. Consequently, the measurement of TCA together with careful pupil alignment and subsequent compensation can improve the functionality of these instruments.

Sammanfattning

Ögat är vårt fönster mot världen, och syn har mätts och studerats i stor utsträckning över åren. Trots detta är forskningen om mänsklig syn oftast begränsad till det centrala synfältet, och i studier av det perifera synfältet korrigeras optiska fel endast över ett smalt våglängdsområde. Denna avhandling vidgar forskningen om vår syn till att inkludera hela det synliga spektrumet över ett stort synfält. Ett brett spektrum innebär att vi måste ta hänsyn till våglängdsberoendet i ljusets brytning i ögat; ögats optik kan därför inte avbilda ett objekt till samma bildläge på näthinnan för alla våglängder, ett fenomen som kallas kromatisk aberration.

Vi presenterar här en ny metod för att mäta mängden transversell kromatisk aberration (TCA) över ögats synfält och visar att ögats TCA ökar linjärt med vinkeln ut i synfältet (ungefär 0,21 bågminuter per grad från 543 nm till 842 nm). Dessutom har vi implementerat adaptiva psykofysiska mätmetoder för att kvantifiera effekten av TCA på central och perifer syn. Våra resultat visar att extra inducerad TCA påverkar den perifera förmågan att upptäcka sinusformade randmönster mer än den centrala förmågan att upplösa motsvarande ränder (mer än 0,05 logMAR per bågminut inducerad TCA i periferin jämfört med 0,03 logMAR/bågminut centralt). Vid utvärdering av perifer syn rekommenderar vi att använda sinusformade randmönster med en sned riktning jämfört med synfältsmeridianen.

Resultaten som presenteras i avhandlingen har klinisk betydelse för att förbättra den perifera synen och är även viktiga för tekniker som avbildar ögats näthinna. För att begränsa den negativa effekt TCA har på synen ska man undvika att inducera extra TCA, t.e.x. när ögats perifera refraktiva fel korrigeras med glasögon för människor med makula degeneration och centralt synfältsbortfall. Vid avbildning av näthinnan ger ögats TCA förskjutningar mellan bilder i olika våglängder. Därför kan mätningar av TCA, tillsammans med välkontrollerad linjering av pupillens position och efterföljande kompensation, förbättra funktionen hos dessa instrument.

List of Papers

This thesis is based on the following Papers:

Paper 1 R. Rosén, L. Lundström, A. P. Venkataraman, **S. Winter**, and P. Unsbo, "Quick contrast sensitivity measurements in the periphery", J. Vis. **14**, 3 (2014).

Paper 2 **S. Winter**, M. Taghi Fathi, A. P. Venkataraman, R. Rosén, A. Seidemann, G. Esser, L. Lundström, and P. Unsbo, "Effect of induced transverse chromatic aberration on peripheral vision", J. Opt. Soc. Am. A **32**, 1764 (2015).

Paper 3 A. P. Venkataraman, **S. Winter**, R. Rosén, and L. Lundström, "Choice of grating orientation for evaluation of peripheral vision", Optom. Vis. Sci. **93**, Epub ahead of print (2016).

Paper 4 C. M. Privitera, R. Sabesan, **S. Winter**, P. Tiruveedhula, and A. Roorda, "Eye-tracking technology for real-time monitoring of transverse chromatic aberration", Opt. Lett. **41**, 1728 (2016).

Paper 5 **S. Winter**, R. Sabesan, P. Tiruveedhula, C. M. Privitera, P. Unsbo, L. Lundström, and A. Roorda, "Transverse chromatic aberration across the visual field of the human eye", manuscript.

The author has contributed to the following paper, which is related to this thesis but has not been included in it.

A A. P. Venkataraman, **S. Winter**, P. Unsbo, and L. Lundström, "Blur adaptation: contrast sensitivity changes and stimulus extent", Vision Res. **110**, 100 (2015).

Contents

List of Abbreviations and Units

2AFC	Two-alternative-forced-choice
2IFC	Two-interval-forced-choice
AOSLO	Adaptive optics scanning laser ophthalmoscope
arcmin	Minutes of arc
BI	Base in orientation of a prism
BO	Base out orientation of a prism
CS	Contrast sensitivity
CSF	Contrast sensitivity function
D	Diopter
F	Power
IR	Infrared
LCA	Longitudinal chromatic aberration
λ	Wavelength
logMAR	Base-10 logarithm of the minimum angle of resolution in minutes of arc
MAR	Minimum angle of resolution
MTF	Modulation transfer function
n	Refractive index
PSF	Point spread function
TCA	Transverse chromatic aberration
V	Abbe number
VA	Visual acuity

Chapter 1

Introduction

Vision is our most developed sense providing vast information about our environment. This thesis is about transverse chromatic aberration and vision. Much research has been performed for enriching the knowledge about the optical and neural processes of vision, which is essential for our understanding of the eye's functionality. However, the in-depth studies about human vision are often either limited to our central visual field or, when extended to the periphery, only correct optical errors related to a narrow spectrum. Extending the knowledge beyond these limits by considering the full visible spectrum over a wide visual field is important.

Since the propagation of light inside the eye is wavelength-dependent, the optics of the eye cannot form an image of a white point source in the same location for all wavelengths. This phenomenon is called chromatic aberration. Even though the visual system has evolved to handle, at least partly, the large chromatic aberration of the eye, the reduction in image quality is still influencing many applications. Wearing high-index spectacles with high power and looking through the edge of the spectacles, one can notice colored fringes at the edges between black and white objects. However, how our vision is influenced by these effects is not completely understood. It is particularly interesting to study the effect of chromatic aberration in the peripheral eye; peripheral vision is important for people suffering from diseases affecting their central vision, such as macular degeneration, leading to central visual field loss. These people rely completely on their peripheral vision, which has larger optical errors than central vision, and benefits from peripheral optical correction [1–3]. Another important motivation to study chromatic aberration across the visual field is to better understand the development of myopia (nearsightedness): the peripheral image quality is suspected to play a major role in sending start/stop signals for the growth of the eye [4]. Furthermore, if one wants to image the retina of a living eye in more than one wavelength [5], the imaging process is always affected by chromatic aberrations. An accurate measurement of the chromatic aberration of the eye gives the possibility to implement a correction that improves image quality.

The following chapters will shed light on the field of transverse chromatic aberration and vision. Chapter 2 gives a brief introduction to the anatomy of the eye. Furthermore, the monochromatic optical errors of the eye and methods to measure and correct them are described. Finally, the peripheral eye and its particularities are explained. Chapter 3 lays a theoretical foundation by introducing the two different types of chromatic aberrations: longitudinal (LCA) and transverse chromatic aberration (TCA). Moreover, suitable eye models that include TCA are discussed, and an estimation of retinal image quality under the influence of TCA is made. Chapter 4 introduces state-of-the-art methods to quantify vision, i.e., contrast sensitivity, visual acuity and Vernier acuity. Chapter 5 connects physical stimuli with their perceptive responses in order to efficiently measure the quantities introduced in Chapter 4. Chapter 6 discusses ways to accurately quantify TCA, and reviews critical issues that influence these TCA measurements. Chapter 7 evaluates the effects of TCA on vision by giving a comparative analysis of the results of the original work. Chapter 8 concludes this thesis by indicating applications and perspective future work.

Chapter 2

The Human Eye

Compared to a camera, the eye may appear as a primitive optical system. However, it is much more flexible in covering a wide range of applications: from low to high light levels, from far to near vision, and from central visual field out in the periphery. This chapter will give a brief introduction to the human eye. The chapter starts with a short description of the anatomy of the eye, the next two sections will explain the monochromatic optical errors and methods to correct for them, and in the last section, the peripheral eye is discussed in more detail.

2.1 Anatomy of the human eye

The process of vision starts with light travelling from the object of interest towards our eyes, which then extract visual information through optical and neural processing. To better understand the eye's function one first needs to be familiar with its structure (see Fig. 2.1) [6, 7].

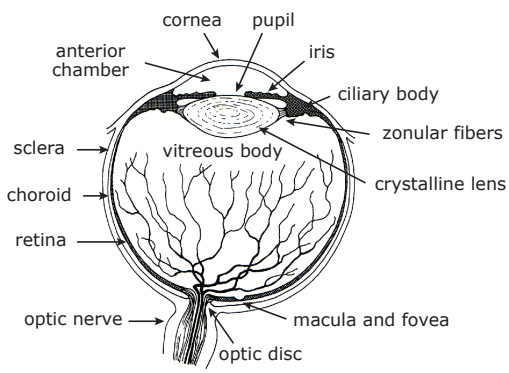

Figure 2.1: Anatomy of the eye (right eye, seen from above). Adapted from Millodot [8].

The eye has an approximately spherical shape and an average length of about 24 mm. The main part of the outer shell of the eye consists of the sclera, a dense, non-transparent tissue. The sclera's main purpose is to protect and hold the eye together. The first surface of the eye that light meets is the **cornea**. The cornea is a transparent tissue that is about 0.5 to 0.6 mm thick and consists of different fiber layers. Furthermore, the cornea is an aspherical surface with a central radius of curvature of about 7.7 mm, and has a refractive index of 1.376. That means that the cornea has a refractive power of around 40 D and accounts for approximately two thirds of the total power of the eye. An important feature of the cornea is the tear film. It smoothes the cornea's surface optically and provides the outer cells of the other corneal layers with nutrients. Directly after the cornea lies the anterior chamber with its aqueous, transparent fluid. The anterior chamber has a length of approximately 3 mm and ensures nutrition of the other parts of the eye. Following the anterior chamber, we find the iris with the pupil in its center.

The **pupil** controls the diameter of the incoming light beam and is therefore the aperture stop of the eye. The pupil size depends on the amount of incoming light and varies typically between 2-8 mm. The center of the pupil varies slightly with its size [9, 10]. The iris is part of the middle layer of the eye (uvea) which consists of iris, ciliary body and choroid. The choroid is a layer covering the inner side of the sclera and provides oxygen and nourishment to the other parts of the eye. The ciliary body with its ciliary muscle is connected to the crystalline lens via the zonular fibers.

The crystalline **lens** is, besides the cornea and the pupil, the third important optical component of the eye and has an approximate power of 20 D. The lens consists of layers of different refractive indexes in an onion-like manner, and thus has a gradient index of refraction structure. To reduce the radius of curvature of the lens and thereby increase its power, the tension in the zonular fibers can be relaxed by contraction of the ciliary muscle. This adjusting process is called accommodation. Accommodation is the eye's ability to focus at varying object distances in order to image the object on the retina. Before the light finally reaches the retina, it passes through the vitreous chamber, which is filled with a clear gel, the vitreous body.

The **retina** is the inner light-sensitive layer of the eye and has a radius of curvature of about 12 mm. The retina consists of several sublayers and one of these at the back of the retina houses the light sensitive cells (photoreceptors). There are two types of photoreceptors, rods and cones. Rods operate at lower levels of illumination whereas cones require higher levels of illumination to generate signals. There are three different types of cones, which have their peak sensitivity in different wavelength ranges, short (S cones), medium (M cones) and long (L cones). Near the center of the retina, the macula (the "yellow spot") is located. The macula has a diameter of 5.5 mm and contains structures that are specialized on high acuity vision. In the center of the macula, there is an avascular dip called fovea that contains the highest density of cones - and therefore giving the highest resolution. The fovea is located in the retina approximately 5° temporal (away from the nose)

and 2° inferior (downwards) from the optical axis of the eye. The generated signal from the rods and cones is transmitted via bipolar and horizontal cells to the retinal ganglion cells. Each ganglion cell has a receptive field of photoreceptors organized in center and surround areas. The signal that a ganglion cell sends depends on the signal combination it receives via the center and the surround of its receptive field. The axons of the ganglion cells form the optical nerve which leaves the eye at the optic disc (located approximately 10°-16° nasally; also called "blind spot" since there are no photoreceptors here). The axons of the ganglion cells are connected to neurons of the lateral geniculate nucleus in the brain where the visual signal information is further processed.

2.2 Monochromatic optical errors of the eye

Ideally, the optics of the eye would be perfectly optimized to give a diffraction limited image on the retina. However, that is not the case for normal pupil sizes and one needs to consider the optical errors that reduce retinal image quality. These optical errors can be divided into two main groups: chromatic and monochromatic aberrations. In general, aberrations mean that not all rays from a point object are striking the same point on the retina to form an image. Chromatic aberrations are caused by the wavelength dependency of the refractive index n, and are explained in more detail in Chapter 3. Monochromatic aberrations occur even if the spectral width of the light is narrowed to one wavelength, and will be discussed in the remainder of this chapter. The monochromatic aberrations can be divided into refractive errors and high-order aberrations.

Refractive errors

Refractive errors, or low-order aberrations, are optical errors that cause the image to be displaced longitudinally from the retina. There are two kinds of low-order aberrations, defocus and astigmatism. If the image displacement is the same for all light rays entering the eye, it is called spherical defocus. There are two main types of defocus: myopia, and hyperopia. Myopia or nearsightedness defines the case when the optical power of the eye is too strong compared to the length of the eye. In contrast, if an eye suffers from hyperopia or farsightedness, then the optical power is too weak for its length. Both myopia and hyperopia can be caused either by erroneous power or length of the eye*. If there is no defocus present, parallel light beams from a distant object will be focused by the optics of the eye onto the retina without any accommodation. This is the desirable case and is called emmetropia.

If the eye suffers from astigmatism, there is a difference in refractive power for rays entering the eye in one principal cross-section (or meridian) compared to the

*Another cause of defocus for nearby objects is presbyopia. This is an aging effect that makes the lens stiffer and thereby reduces the ability of the eye to accommodate.

perpendicular principal cross-section. This difference in power results in two line foci, one for each principal meridian, instead of one focal point. Astigmatism can arise, for example, because of a toroidal shape of the cornea, i.e., different radii of curvature in different meridians resulting in a difference in refractive power between these two meridians. Astigmatism is also induced if the object of interest is located off-axis. The off-axis location of the object causes a difference in incidence angle between meridians, resulting again in a difference of power. This kind of astigmatism is referred to as off-axis astigmatism. For off-axis astigmatism, the orientation of the two principal meridians, usually denoted as tangential and sagittal plane, is connected to the off-axis direction. As can be seen in Fig. 2.2, the tangential plane includes the chief ray and the optical axis of the eye, while the sagittal plane is located perpendicular to the tangential plane and only includes the chief ray. The power of the eye will be higher in the tangential meridian compared to the sagittal meridian, again leading to two line foci. In both kinds of astigmatism, the smallest cross-section of the blur circle (the circle of least confusion) is located between the two line foci.

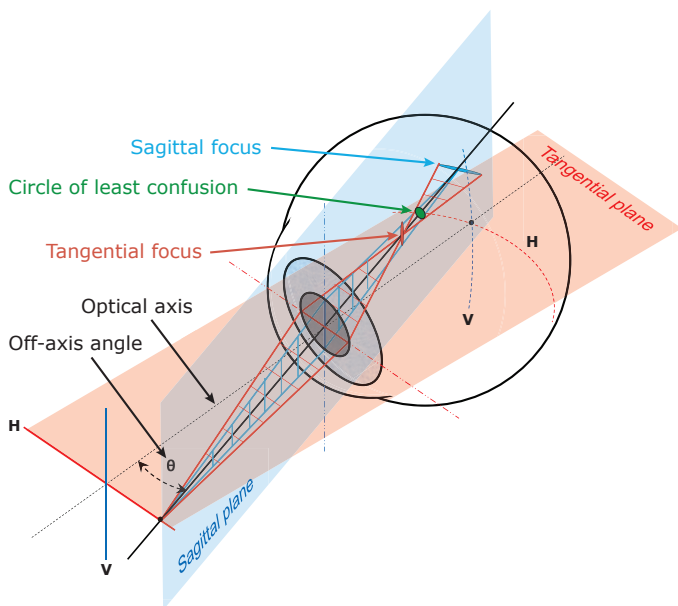

Figure 2.2: Off-axis astigmatism in the eye. Off-axis astigmatism arises when light enters the eye in an off-axis angle. The consequence is the presence of two line foci instead of one focal point. The smallest cross-section of the blur circle (circle of least confusion) is located inbetween the two line foci. Adapted from Lewis [11].

High-order aberrations

High-order aberrations are more irregular optical errors than refractive errors, meaning that rays through different parts of the pupil will not meet in one image nor in two line foci. Since the propagation of the rays inside the eye is not directly accessible, high-order aberrations are often measured by sending light into the eye and analysing the back-reflected light from a small illuminated spot on the retina. The aberrations of the eye are manifested in the outgoing wavefront, which shows the difference in how the rays that exit through different parts of the pupil are refracted, as can be seen in the left part of Fig. 2.3. Therefore, high-order aberrations can be measured as deviations from a perfectly flat wavefront. In the eye, these wavefront aberrations are commonly expressed as Zernike coefficients* [12–14]. The shape of a wavefront can then be described as the sum of Zernike coefficients c_n^m multiplied by the corresponding Zernike polynomials Z_n^m

$$W(\rho,\theta) = \sum_{m,n} c_n^m Z_n^m(\rho,\theta) \tag{2.1}$$

The Zernike coefficients c_n^m are typically measured in µm and are dependent on pupil size. The Zernike polynomials Z_n^m are a product of a radial polynomial with a trigonometric function and a normalization factor. An overview of the different wavefront shapes corresponding to the different Zernike polynomials can be seen in Fig. 2.4.

Spherical aberration is the most common high-order aberration in the eye. It is an optical error where the rays that enter through the edges of the pupil are refracted more than the rays through the center of the pupil. This results in different focus positions depending on ray height. The blur in the retinal image due to spherical aberration is thereby strongly dependent on the size of the pupil and spherical aberration mostly manifests as halo phenomena in night vision. Another common high-order aberration in the eye is coma, which gives a comet-like tail in the image of a point source. There are also other high-order aberrations in the eye which are not present in a rotationally symmetric system such as trefoil.

2.3 Adaptive optics correction of aberrations

An important goal in vision science and optometry is to find appropriate optical corrections for the optical errors of the eye with the aim of improving retinal image quality. Low-order aberrations in the fovea can be measured by traditional subjective refraction and be corrected by spectacles, contact lenses or trial lenses. To also measure high-order aberrations a higher technical investment is required, but can be realized with the help of, e.g., a Hartmann-Shack sensor (see Fig. 2.3) that evaluates the outgoing, aberrated wavefront.

*This should not be confused with the classification according to Seidel theory; particularly the characterization what order an aberration has, changes in between the two classifications.

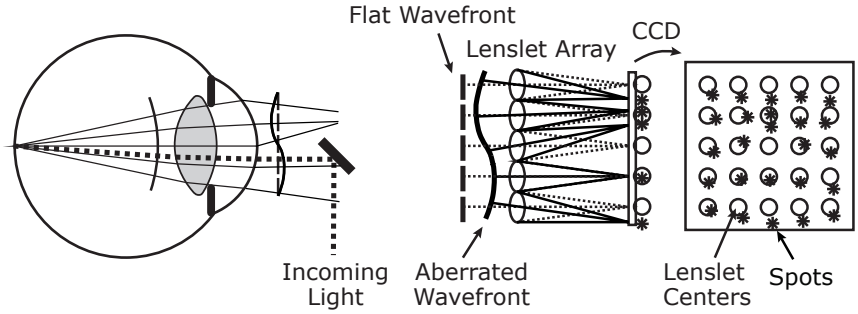

Figure 2.3: The principle of a Hartmann-Shack wavefront sensor for estimating ocular aberrations. Left: A retinal spot is illuminated by a narrow, collimated IR laser beam. The laser beam is reflected diffusely, affected by the optical errors of the eye, and leaves the eye with an aberrated wavefront. Right: After imaging the pupil plane of the eye onto the lenslet array of the sensor, the aberrated wavefront is divided into smaller sections and focused by the lenslets. The slope of the wavefront at a particular location in the pupil is represented by the shift of the spot behind the lenslets from the projected lenslet centers. Aberrations are exaggerated for better clarity. Adapted from Lundström [15].

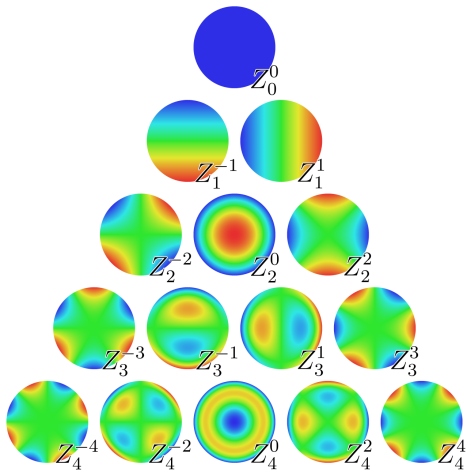

Figure 2.4: The monochromatic aberrations expressed as Zernike polynomials Z_n^m (first fifteen shown). Monochromatic aberrations can be divided into low-order aberrations (first three rows) and high-order aberrations (row four and higher indexes). The low-order aberrations are defocus (Z_2^0) and astigmatism (Z_2^{-2} and Z_2^2). The most important high-order aberrations in the eye are spherical aberration (Z_0^4), coma (Z_3^{-1} and Z_3^1), and trefoil (Z_3^{-3} and Z_3^3). Adapted from Rocchini [16], licensed under CC-BY-3.0.

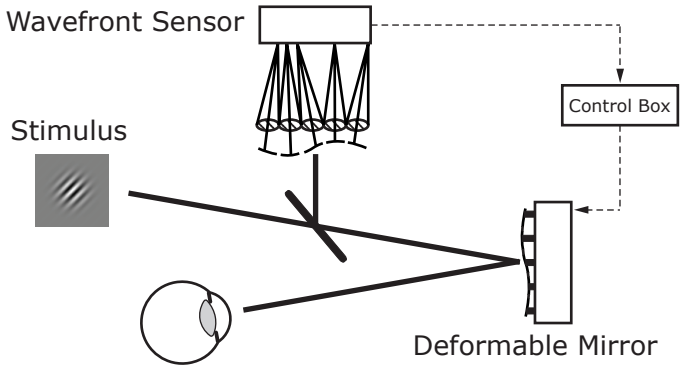

Figure 2.5: Adaptive optics (AO) system. With an AO system, one can measure and correct monochromatic ocular aberrations while simultaneously presenting visual stimuli to the subject's eye. The aberrations are measured by the wavefront sensor. The control box processes the input signal from the wavefront sensor and sends a feedback signal to the deformable mirror. The deformable mirror corrects the wavefront that can again be measured by the wavefront sensor. While the optical correction is running in closed loop, visual stimuli can be presented on the stimuli presentation system as applied in Paper 1, 2, and 3. Adapted from Lundström [15].

In adaptive optics (AO) systems, the information obtained from a wavefront sensor can be sent to a deformable mirror that modulates the wavefront and corrects the present aberrations (see Fig. 2.5). The quality of the correction can be judged by calculating the root-mean-square value (RMS) of the corrected wavefront. Due to the orthonormality of the Zernike polynomials the total RMS value of a wavefront can be written as the square root of the sum of squares of the individual Zernike coefficients [13, 14]:

$$\mathrm{RMS} = \sqrt{\sum_{m,n} (c_n^m)^2} \tag{2.2}$$

With successful AO correction, vision can be studied under well-controlled image quality: via the deformable mirror, the subject sees various visual stimuli, shown by the stimuli presentation system, at the same time as the wavefront sensor measures the remaining optical errors (see, for example, Paper 1, 2 and 3).

Just as the image quality on the retina can be limited by the eye's aberrations, these aberrations can also limit the resolution of images of the retina itself. Adaptive optics can be used to bypass these limitations and record high resolution retinal images with, e.g., an adaptive optics scanning laser ophthalmoscope (AOSLO) [5, 17]. In an AOSLO, a laser beam scans the retina point by point. During the scan, the wavefront of the beam is modulated by an deformable mirror to compensate for the monochromatic aberrations of the eye as measured by a wavefront sensor. The

reflected light signal is then registered in photomultiplier tubes. Such an AOSLO has been utilized in Paper 4 and 5.

2.4 The peripheral eye

In this section we take a closer look at some particularities of the peripheral eye. Here in this thesis, the "peripheral" eye means that we consider all visual angles from just outside of the macula; typical off-axis angles used in this thesis are 10-20°. The four commonly selected directions of eccentricity are nasally (closer to the nose), temporally (away from the nose), superior (above the horizontal meridian), and inferior (below the horizontal meridian).

Optical limits

The image quality in the eye decreases with increasing off-axis angle. The main monochromatic optical limits of the peripheral eye are refractive errors, i.e., the low-order aberrations defocus and off-axis astigmatism, and the high-order aberration coma. As explained before, off-axis astigmatism emerges from a difference in the angle of incidence in between meridians due to the off-axis position. Off-axis astigmatism increases quadratically with the off-axis angle but is also influenced by the foveal astigmatism and needs to be measured individually [18–20]. Defocus is also not necessarily the same over the whole visual field; the focal power and/or the length of the eye may change for different eccentricities leading to peripheral refractive errors [21]. Coma is the dominant high-order aberration in the periphery showing a linear dependency with the off-axis angle [19,22,23]. Spherical aberration is influenced by the shape of the cornea and the lens, but does not increase with off-axis angle [19, 24].

Neural limits

Apart from the peripheral optical errors, we also need to consider an anatomical change from the fovea to the periphery of dramatic impact. As can be seen in Fig. 2.6, the density of photoreceptors varies with eccentricity as does the density of ganglion cells. In the central fovea, one ganglion cell is connected to one cone, but in the periphery several cones connect to one and the same ganglion cell. This will cause some visual functions to differ much more for peripheral vision than for foveal vision as explained in Chapter 4. Furthermore, the peripheral ganglion cells are more sensitive to grating stimuli with the lines pointing radially towards the center of the visual field (parallel gratings) than to perpendicular line orientations (perpendicular gratings, see Fig. 7.4 and Paper 3), which is called the meridional effect. Note that this orientation preference in the periphery is different from the foveal one, called oblique effect (see Paper 3, Campbell et al. [25], and Rovamo et al. [26]).

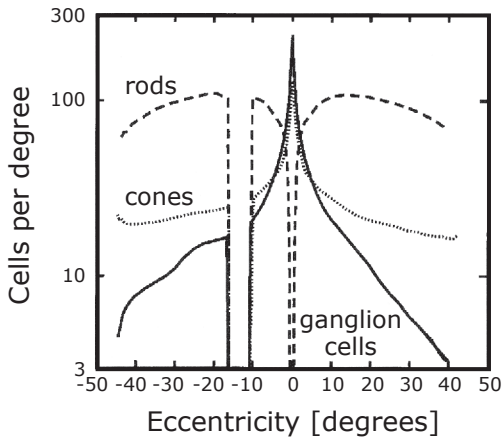

Figure 2.6: The density of rods, cones and ganglion cells in the human retina as a function of eccentricity from the fovea. The optic disc ("blind spot") is located in the nasal retina (empty area). Adapted from Geisler and Banks [27] who in turn used data from Curcio et al. [28, 29].

Chapter 3

Theory of Chromatic Aberration

This chapter will give an overview of the origin of chromatic aberrations. It will focus on transverse chromatic aberration and its variation over the visual field. Furthermore, it will review how TCA can be included in eye models. To estimate the influence of chromatic aberrations on the optical quality of the retinal image, unpublished simulation data on the magnitude of TCA is presented.

3.1 Fundamentals of chromatic aberrations

The interaction between light and matter is described by the refractive index n, defined as the ratio between the speed of light in vacuum and in the material. Chromatic aberration is caused by **dispersion**, meaning that the refractive index of a medium is a function of the wavelength ($n = n(\lambda)$). This wavelength dependency can be seen for the different media of the human eye in Fig. 3.1.

If we assume the simplest possible eye model, a **reduced eye model**, there is only one spherical refracting surface, the cornea, separating air from the dispersive ocular media. For the paraxial power of this spherical surface we can write

$$F_{\mathrm{d}} = \frac{n'_{\mathrm{d}} - 1}{r_{\mathrm{cornea}}} \tag{3.1}$$

with the refractive index within the eye for green light n'_{d} ($\lambda_{\mathrm{d}} = 587.6$ nm), and the corneal radius of curvature r_{cornea}. The difference in power between blue ($\lambda_{\mathrm{F}} = 486.1$ nm) and red ($\lambda_{\mathrm{C}} = 656.3$ nm) light, ΔF, is then given by

$$\Delta F = F_{\mathrm{F}} - F_{\mathrm{C}} = \frac{n'_{\mathrm{F}} - n'_{\mathrm{C}}}{r_{\mathrm{cornea}}} \tag{3.2}$$

and the ratio $\frac{F_{\mathrm{d}}}{\Delta F}$ can be expressed as

$$\frac{F_{\mathrm{d}}}{\Delta F} = \frac{n'_{\mathrm{d}} - 1}{n'_{\mathrm{F}} - n'_{\mathrm{C}}} = V_{\mathrm{d}} \tag{3.3}$$

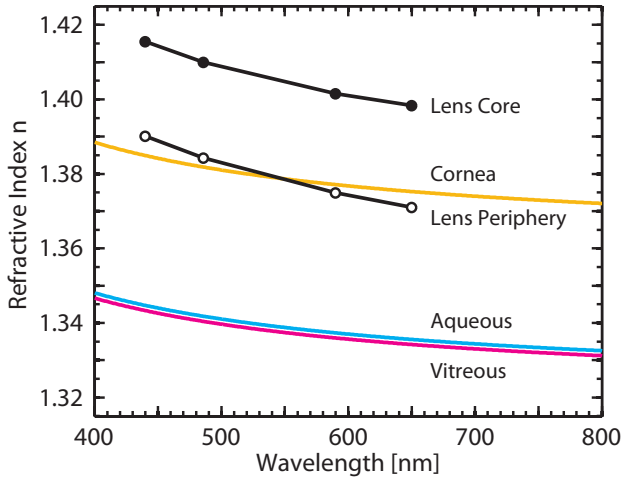

Figure 3.1: Dispersion in the human eye. The refractive index of lens (core - closed circles, periphery - open circles), cornea (orange), aqueous (cyan) and vitreous (magenta) depends on wavelength. Data for cornea, aqueous and vitreous from Le Grand [30], and for the lens from Sivak and Mandelman [31].

with the well-known **Abbe number** V_d. In the reduced eye model one sets $F_\mathrm{d} = +60$ D, $n'_\mathrm{d} = 1.336$. With the Abbe number for water of $V_\mathrm{d} = 55$ we calculate

$$\Delta F = \frac{F_\mathrm{d}}{V_\mathrm{d}} = \frac{60}{55} \approx 1.09 \text{ D} \tag{3.4}$$

as the difference in power, describing how much more short wavelengths (blue) are refracted than longer wavelengths (red). When describing the chromatic aberrations of the eye, two kinds are commonly distinguished: **longitudinal chromatic aberration (LCA)** and **transverse chromatic aberration (TCA)**.

Longitudinal chromatic aberration

Longitudinal, or axial, chromatic aberration causes a more myopic refractive error for shorter than for longer wavelengths. Furthermore, LCA is present even for on-axis objects as can be seen in Fig. 3.2. Since the optical path length of the eye also varies with wavelength, the chromatic difference in refraction (CDRx) is lower than the difference in power. The CDRx is approximately -0.82 D, and will in the paraxial approximation be independent of the off-axis angle (assuming the same length of the eye also in the periphery). This independence of off-axis angle was also found in two studies of peripheral LCA [32, 33]. Note that the blur on the retina due to LCA is dependent on pupil size.

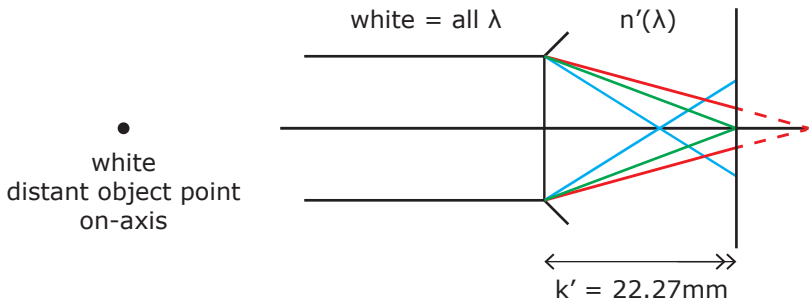

Figure 3.2: Longitudinal chromatic aberration (LCA) in a reduced eye model.

Transverse chromatic aberration

In contrast, transverse, or lateral, chromatic aberration causes an angular offset between the chief rays of different wavelengths (Fig. 3.3). For point sources, this angular offset results in different retinal image positions (**chromatic difference in position (CDP)**), whereas for extended objects the magnification will differ depending on wavelength (**chromatic difference in magnification (CDM)**). TCA is zero for objects on the optical axis, but increases with off-axis angle. Furthermore, the angular offset is independent of the size of the pupil. However, a de-centered pupil will change the magnitude of TCA as there will be a different chief ray (see also Paper 4).

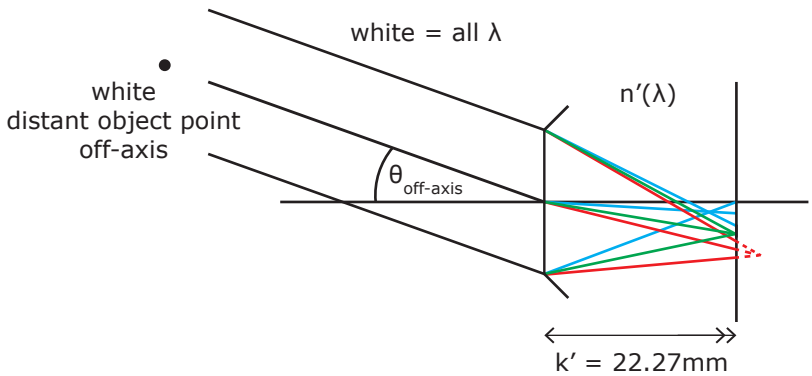

Figure 3.3: Transverse chromatic aberration (TCA) in a reduced eye model.

3.2 Modeling the TCA of the human eye

The reduced eye model as described in the previous section gives a qualitative explanation to the origin of ocular chromatic aberration. However, the reduced eye model is a much simplified model and will give unrealistic magnitudes of TCA if used for calculations. One important aspect of finding a good chromatic eye model is an appropriate description of the refractive index. The relationship between wavelength λ and refractive index n is commonly described by empiric formulae. One of them is the Hartmann-Cornu formula [34, 35]:

$$n = n_0 + \frac{c}{(\lambda - \lambda_0)^\alpha} \tag{3.5}$$

with n_0, λ_0, c and α being constants in the relationship of n depending on λ (Note: c is not the speed of light). The above mentioned formula by Hartmann is a generalization of a simpler formula given earlier by Cornu to analyze the solar spectrum in the UV range after passage through a prism [35]. The Cornu formula describes the special case of $\alpha = 1$ [30, 34].

Atchison and Smith studied the feasibility of several dispersion formulae for the application in the eye: although the Cornu formula may slightly underestimate the magnitude of dispersion in the infrared part of the spectrum and is not favoured by Atchison and Smith, it still seems to be a reasonable approximation for the refractive index in the eye up to 900 nm [36].

There is a large number of different eye models trying to give reasonable representations of different optical parameters of the human eye. However, the work of Thibos and collaborators with the Chromatic Eye and the Indiana Eye is of special interest since they specifically worked on modeling ocular TCA [37–39]. In their work, Thibos et al. made the following changes in the previously described reduced eye model:

1. The pupil was moved from the reduced surface into the eye, to give a more realistic description of the entrance pupil of the eye, and of the passing of the chief ray through the reduced surface for off-axis angles.

2. The retina became spherical in order to be able to predict peripheral image quality.

3. The dispersion in the ocular media was described by the Cornu formula, and its parameters were obtained by fitting to experimental data.

4. The fovea was placed off the optical axis of the eye model to correctly represent foveal TCA as non-zero (only in the Chromatic Eye).

5. Furthermore, the corneal shape was changed to be aspheric, to realistically model both TCA and spherical aberration.

The properties of these chromatic eye models were taken into consideration in Paper 5 for building a physical eye model.

3.3 Simulations of image quality with chromatic aberrations

To estimate the impact of chromatic aberrations on image quality, we simulated the modulation transfer function (MTF), spot ray diagrams illustrating the point spread function (PSF), and TCA over the visual field in a commercial optical design software (Zemax OpticStudio). The results of the simulations are shown in Figs. 3.4 to 3.6.

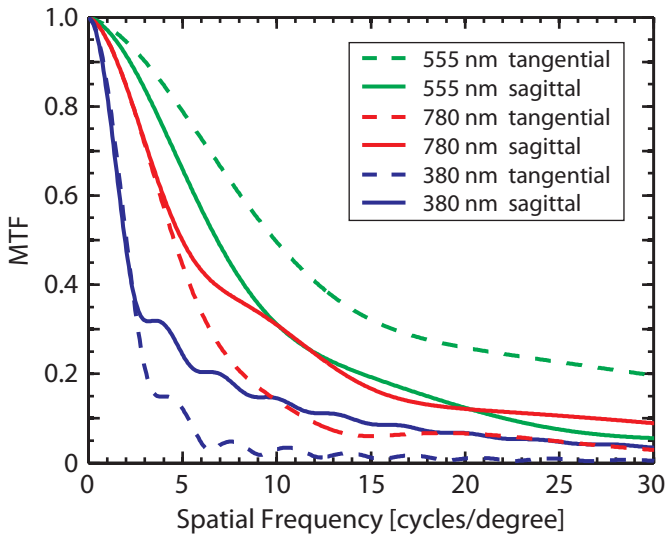

Figure 3.4: Modulation transfer function (MTF) in the fovea for a chromatic model eye. The MTF was calculated with a 3 mm pupil for the wavelengths 380 nm (blue), 555 nm (green) and 780 nm (red). Sagittal and tangential planes are shown as solid and dashed lines, respectively. Unpublished data.

The following parameters are applied in the simulations: refractive index for wavelength λ in microns, as calculated from the Cornu formula,

$$n(\lambda) = a + \frac{b}{\lambda - c} \tag{3.6}$$

with a=1.320535, b=0.004685, c= 0.214102; corneal radius of curvature to be 5.55 mm; conic constant $k = -\epsilon^2 = -0.563$; axial position of the physical pupil 1.91 mm away from the vertex of the reduced surface, and a retinal radius of curvature of -11.00 mm (all given by Thibos et al. [39]). The pupil diameter, was chosen to be 3 mm since this pupil size gives, on average, best resolution acuity [6]

and is representative for daylight luminance conditions. The pupil was centered on the optical axis. The fovea was moved from the optical axis by 5° temporal and 2° inferior on the retina [6]. The eye was made paraxially emmetropic for the wavelength 555 nm in the fovea, which resulted in an eye length of 22.14 mm.

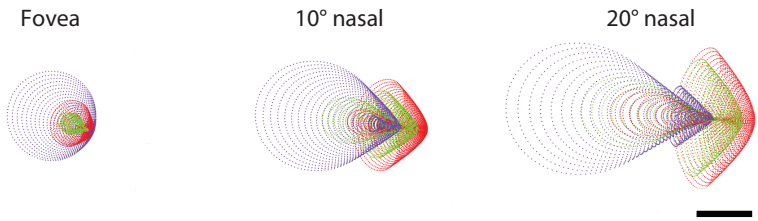

Figure 3.5: Spot ray diagram illustrating the point spread function for a chromatic eye model. Here shown with a 3 mm pupil in the fovea, in 10°, and in 20° nasal visual field (380 nm - blue, 555 nm - green, 780 nm - red). The eye was made emmetropic for 555 nm. Scale bar corresponds to 70 µm. Unpublished data.

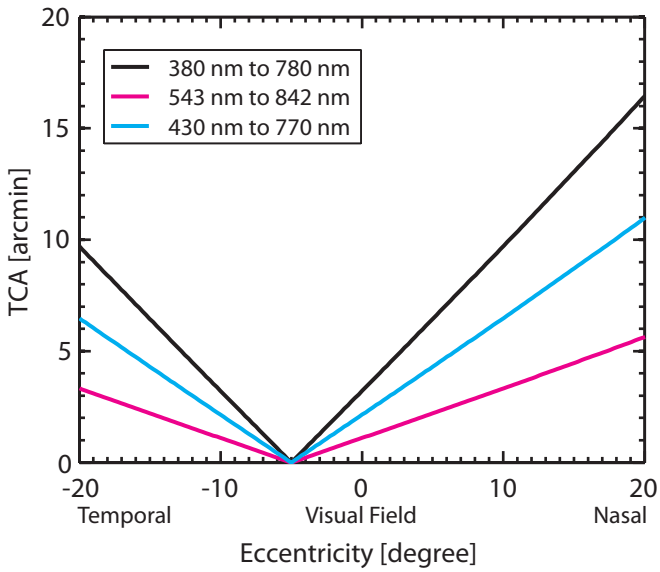

Figure 3.6: Simulated TCA in object space of the eye. TCA was simulated in a chromatic eye model over the horizontal visual field for the visual spectrum 380 nm to 780 nm (black), 543 nm to 842 nm (magenta) as used in Paper 5, and 430 nm to 770 nm (cyan) as used by Thibos [37]. Pupil aperture was placed 1.91 mm behind the cornea, and the dispersion of the ocular media was modeled with the Cornu formula. Unpublished data.

As can be seen in Fig. 3.4, the MTF for the modeled eye is wavelength-dependent. The difference of the MTF curve in between wavelengths is most noticeable in the fovea due to LCA. Furthermore, the MTF decreases with off-axis angle (not shown). Off-axis, the MTF is dominated by refractive errors.

To also visualize the effect of TCA on image quality, spot ray diagrams are plotted in Fig. 3.5. As can be clearly seen, TCA is increasing with off-axis angle. Furthermore, the increasing effect of coma and astigmatism can also be noticed.

Foveal TCA for the visual spectrum (380 nm to 780 nm) is estimated to be 3.2 arcmin (see black curve in Fig. 3.6). Off-axis, the TCA increases nearly linearly with a rate of approximately 0.66 arcmin/degree. For the other spectra, the rate is 0.44 arcmin/degree (430 nm to 770 nm) and 0.23 arcmin/degree (543 nm to 842 nm). Clearly, the TCA is not symmetric to the fovea, since the fovea is displaced from the optical axis. The TCA of this simplified model with a central pupil is zero on the optical axis, which corresponds in the horizontal meridian to the 5° temporal visual field.

Chapter 4

Quantifying Vision

For the quantification and evaluation of vision, adequate techniques are required as in any other field of science. Many of us probably remember the letter chart from our last visit to an eye doctor's clinic. Letter charts are used to estimate the smallest detail size that one can still see. However, these letter charts are only evaluating one specialized aspect of vision, i.e., high contrast resolution. This chapter focuses on three different measures of vision: contrast sensitivity, visual acuity, and Vernier acuity.

In Paper 1, 2, and 3, contrast sensitivity and visual acuity were implemented with sinusoidal gratings in order to judge both central and peripheral vision. The advantage of utilizing sinusoidal gratings is that they consist of only one single spatial frequency and that all other objects can be described by a combination of gratings with different spatial frequencies and contrasts. If one knows the object (i.e., its spatial frequency content) and the optical transfer function of the eye, then the retinal image quality can be described by Fourier optics [40]. Furthermore, there are many indications that the neural visual system is also operating in the spatial frequency domain [41].

4.1 Contrast sensitivity

Contrast sensitivity is one way of quantifying vision, but to talk about contrast sensitivity, one first needs to define contrast. In this thesis and the connected publications, the contrast of a grating is defined by the Michelson contrast C_{M}:

$$C_{\mathrm{M}} = \frac{L_{\max} - L_{\min}}{L_{\max} + L_{\min}} \tag{4.1}$$

with $L_{\min}$ and $L_{\max}$ being the minimum and maximum luminance of the grating. Contrast sensitivity (CS) is then defined as the inverse of the contrast-threshold:

$$\mathrm{CS} = \frac{1}{C_{\mathrm{threshold}}} \tag{4.2}$$

This means that the lower the contrast threshold that one can see, the higher the CS will be, i.e., better vision. To measure contrast sensitivity, a subject can be asked to resolve the orientation of a sinusoidal grating of varying contrast, but with fixed spatial frequency. The contrast sensitivity function (CSF) visualizes the contrast sensitivity over a range of spatial frequencies; an example from one subject (subject 2, Paper 1), measured at different visual field eccentricities, can be seen in Fig. 4.1. In the fovea (black curve), spatial frequencies of about 5 to 6 cycles/degree give the maximum contrast sensitivity at high photopic luminance, but shift to lower frequencies with lower luminance [41]. The reduction in CS for high spatial frequencies is mainly of optical origin due to aberrations, scattering and diffraction. However, the decrease for lower spatial frequencies is due to neural reasons, i.e., inhibitory processes in the retinal ganglion cells between the surround and the center of the receptive fields [41]. In the periphery (colored curves in Fig. 4.1), the eye is less sensitive to contrast and the peak contrast sensitivity is shifted towards lower spatial frequencies. The reason for this is an increase of receptive field size for the peripheral ganglion cells. More specifically, this increase of receptive field size in the periphery comes from the neural sampling limitation of several photoreceptors sharing one ganglion cell.

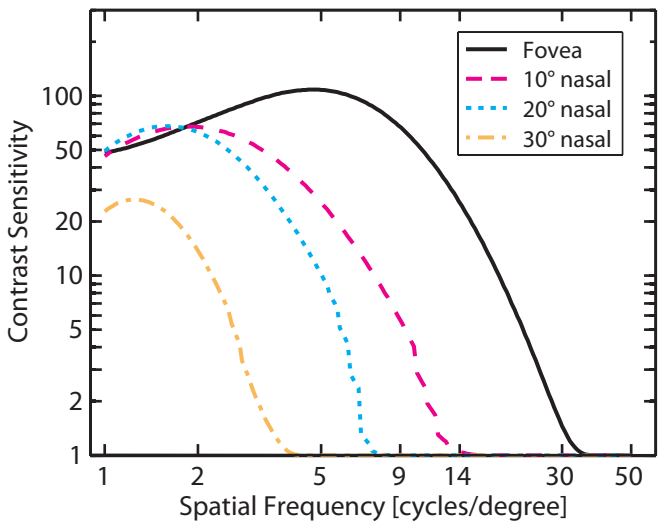

Figure 4.1: Contrast sensitivity (CS) function in the fovea (black solid), 10° (magenta dashed), 20° (blue dotted), and 30° (orange dashdot) nasal visual field. For increasing eccentricity, the maximum CS decreases and the peak sensitivity is shifted towards lower spatial frequencies. CS was measured with the quick CSF method (see Chapter 5). Data from Paper 1, subject 2 (periphery) and unpublished data from the same subject (fovea).

4.2 Visual acuity

Visual acuity describes the ability to see and correctly identify fine image details. To measure visual acuity a subject can be asked to, e.g., discriminate the orientation of a grating of varying spatial frequency or identify a letter with varying size, but with fixed contrast. The smallest detail size one can resolve is the minimum angle of resolution (MAR), and it is measured in minutes of arc (see Fig. 4.2). Other common ways to express the visual resolution limit are the decimal visual acuity VA = 1/MAR, the frequency cutoff in cycles per degree $\nu = 30/\text{MAR}$ and $\text{logMAR} = \log_{10}(\text{MAR})$. Normal foveal vision would be VA 1.0 and above. The visual acuity for high contrast stimuli (100% contrast) also corresponds to the cutoff frequency in the contrast sensitivity function (cf. Fig. 4.1).

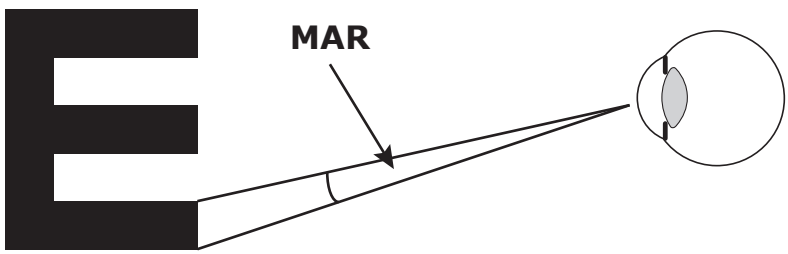

Figure 4.2: The minimum angle of resolution (MAR). The MAR is a measure of visual acuity and the finest detail an eye can resolve (here shown with the letter E, for a grating this would correspond to half of the grating period). Typically, the MAR is measured in minutes of arc (arcmin).

Resolution acuity

Both contrast sensitivity and visual acuity are described above as resolution tasks, i.e., the subject was required to identify the details of the stimulus. One could intuitively think that the maximum resolution limit is determined by the photoreceptor density in the retina. However, with optimum retinal image quality, resolution would be limited by the density of the ganglion cells, as this density is lower than the photoreceptor density [42,43]. Since the ganglion cell density is decreasing with increasing visual angle, the resolution acuity is also decreasing in the peripheral visual field.

Detection acuity

If the spatial frequency in the retinal image is higher than the sampling density of the retina, the presence of the stimulus can still be perceived, but not resolved.

This is called detection acuity and can be measured similarly to resolution as the minimum angle of detection. Whether detection acuity differs from resolution depends on the spatial frequency and the sampling density. If the Nyquist criterion is satisfied at threshold, i.e., if the sampling density is more than twice as high as the image frequency [44], then the sampled image will be a correct representation of the retinal image and resolution and detection acuity will be the same (see Fig. 4.3, upper row). Conversely, if the spatial frequency is too high for the sampling density, the sampled image will be a Moiré pattern of the original image that can be detected but not resolved (see Fig. 4.3, lower row). This effect is called aliasing. Aliasing is present in foveal and peripheral vision, however, foveal aliasing is often hidden by the optical errors of the eye.

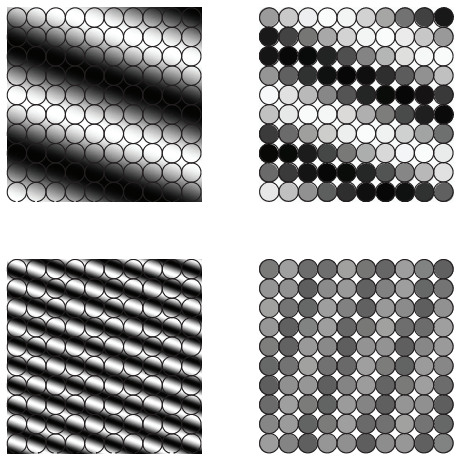

Figure 4.3: The concept of aliasing in the eye. Left: A sinusoidal grating is imaged on the retina with discrete sampling by the photoreceptors (array of circles). Right: The response signal given by the photoreceptors. Upper: The imaged grating has a low enough spatial frequency to be resolved by the photoreceptors according to the Nyquist criterion [44]. Lower: The imaged high-frequency grating creates a photoreceptor response where it is still possible to detect a pattern. However, neither the spatial frequency nor the grating's orientation are resolved correctly. Remark: In a real eye, the retinal sampling is more irregular.

For peripheral vision, aliasing leads to a higher detection acuity than resolution acuity for high-contrast gratings [45]. Peripheral detection will thereby be contrast-limited also above the Nyquist frequency and is therefore more sensitive to reduction in image quality than peripheral resolution. Considering the contrast sensitivity function, this will show up as an aliasing zone (Fig. 4.4).

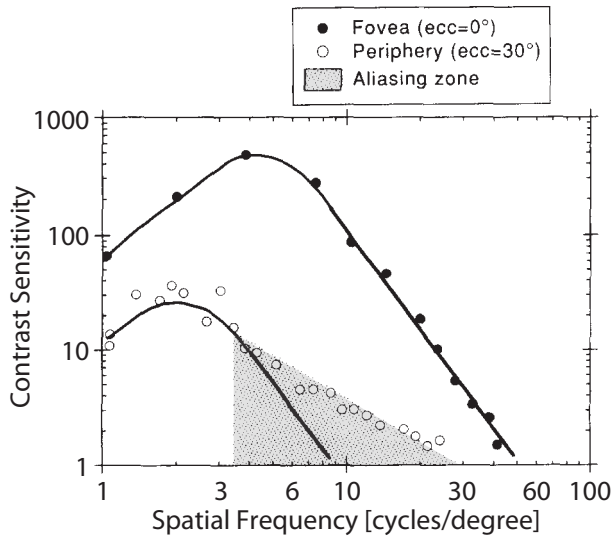

Figure 4.4: Contrast sensitivity (CS) and aliasing. CS function is shown for foveal (closed circles) and peripheral (open circles) grating detection. In the periphery, there exists an aliasing zone where gratings can still be detected but not resolved (shaded area). To compare the measured peripheral CS with the foveal data, the curve of the foveal fit was shifted left and down. Reproduced from Thibos et al. [46] with permission from Elsevier.

4.3 Vernier acuity

Vernier acuity describes the ability to detect the misalignment of two objects (e.g., two points, or two lines). The threshold of Vernier acuity in foveal vision is significantly better than resolution acuity and is used in everyday life when reading a caliper with a Vernier scale*. Vernier acuity can also be used for the measurement of TCA [47]. From the displacement of two black bars on red and blue background, the magnitude of perceived TCA in the fovea can be calculated (see Fig. 4.5 and Paper 2). However, Vernier acuity degrades with eccentricity in peripheral vision [48], and this degradation is even faster than for resolution acuity [49, 50]. This might explain the rather large variability in the measurement data of Ogboso and Bedell, when they attempted to measure the magnitude of transverse chromatic aberration in the periphery [51] (see also Chapter 6). The degradation of Vernier

*The Vernier scale is named after Pierre Vernier. Vernier described the scale for the application in astronomical instruments in his book "La construction, l'usage, et les propriétés du quadrant nouveau de mathématique", 1631.

acuity in the periphery is also the reason why in Paper 2 the Vernier alignment method was applied in foveal but not in peripheral vision.

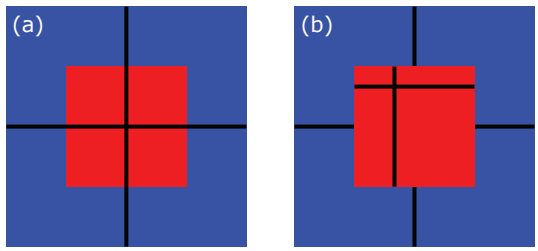

Figure 4.5: Vernier alignment method for the measurement of TCA in Paper 2. A small red square is located in the middle of a larger blue square. A cross of black bars is placed on top of both squares. (a) Although the black bars are completely aligned, TCA will cause the eye to see a tiny step on the edge between the red and the blue background of the bars. (b) The black bars in the center are purposely misaligned. The subject is asked to adjust the bars in the center until they appear to be aligned. From the remaining displacement, one can calculate how much TCA the subject perceives.

Chapter 5

Psychophysical Evaluation of Vision

Psychophysics is the field of science where the perceptional response to a physical stimulus is measured. In vision science the aim of a psychophysical procedure is most often to find a threshold value of the physical stimulus, at which the stimulus can just barely be seen. A typical task would be to ask the subject whether or not (s)he can read letters of a certain size. The challenge is to ask the right questions to get the most information about the threshold one wants to measure. In the following chapter the psychometric function, different response designs, and classical psychophysical procedures are described (for a more thorough description the reader is referred to the book of Norten et al. [52] and Treutwein's minireview [53]). Moreover, the chapter explains adaptive psychophysical procedures, which were implemented in Paper 1, 2 and 3 to efficiently evaluate central and peripheral vision. The chapter concludes by elucidating the design of the visual stimuli implemented in our experiments.

5.1 The psychometric function

An important way to quantify the relationship between stimuli and response is the **frequency-of-seeing curve** or **psychometric function** (see Fig. 5.1). The psychometric function shows the percentage of correct answers depending on the stimulus strength. Stimulus strength is hereby an umbrella term for different stimulus properties that can be (controllably) varied in the measurement (e.g., size or contrast). The stimulus properties are changing on the x-axis from difficult-to-see on the left to easy-to-see on the right. The transition between "can never see" and "can always see" is not a sharp one. Therefore, there is a transition zone of a certain width that gives the psychometric function its typical s-shape (see Fig. 5.1). The **threshold** of the psychometric function reports the stimulus strength corresponding to a certain percentage of correct answers (in Fig. 5.1 this is set to 72.5%).

As such, the threshold defines the location of the psychometric function along the x-axis.

Even if the stimulus strength is far to the right in Fig. 5.1 and should in principle always be seen, there is a probability that one does not answer correctly. This is called the **lapse rate** (or false negative error), and is limiting the maximum value of the psychometric function. Possible reasons for the lapses are, for example, blinks, poor tear film or loss of concentration. In Paper 1, 2, and 3 the lapse rate was set to 5% which means that the subject was expected to make 2-3 mistakes during 50 stimulus presentations (trials). The lapse rate can be reduced by accompanying the visual stimuli by an auditory cue. Similar to the lapse rate, there will also be a certain percentage of correct answers even though the stimulus is not sensed. This is called the **guess rate** (or false positive) and gives the minimum value of the psychometric function. In practice, the minimum value of the psychometric function can also be affected by the subject, as (s)he may avoid guessing and instead report that the stimulus is not seen. As the threshold is usually defined to be halfway in between the minimum and the maximum value of the psychometric function, it is therefore important to control the way the subject is required to respond, i.e., the task of the subject.

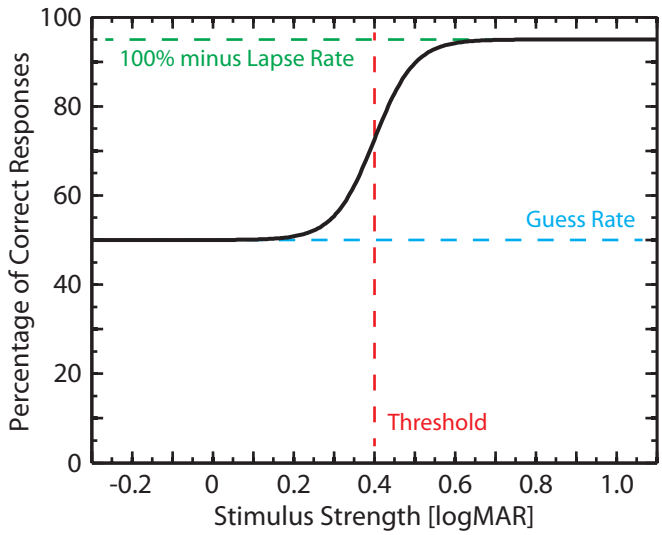

Figure 5.1: Psychometric function. The psychometric function shows the frequency of seeing for a certain stimulus strength. Guess rate (50%) and lapse rate (5%) determine the lower and upper limit of the curve. The threshold (0.4 logMAR) is estimated halfway (72.5%) between the guess rate and the 100% level reduced by the lapse rate (95%). Guess rate and lapse rate values are shown as implemented in Paper 2, the estimated threshold is shown exemplarily.

5.2 The task of the subject

One of the main design choices for a psychophysical experiment is the task to be performed by the subject. For example, the two common tasks of yes/no (see/not see) and forced-choice differ in control of the guess rate. In a **yes/no task** the subject gets presented a certain stimulus strength and is asked whether or not, (s)he can see it. Therefore, yes/no tasks are at risk of subject-bias, e.g., to please the experimenter with an expected result, and do not control the guess rate. It is thereby difficult to know the level of correct responses for the threshold in a yes/no task. In contrast, **forced-choice** tasks offer a control over the guess rate. In forced-choice tasks, two or more response options are given and the subject has to make a choice between them (e.g., in the resolution task of Paper 2, the subject chose between two different orientations of a grating). The guess rate in forced choice tasks is one over the number of alternatives (for 2-alternatives-forced-choice (2AFC) the guess rate is 50%, for 4AFC it is 25%, and so on). Obviously, increasing the number of alternatives in the forced-choice decreases the guess rate, but the complexity of the task for the subject is being raised at the same time. Therefore, a balance between guess rate and complexity has to be found in the experimental design. Furthermore, the control over the guess rate also gives knowledge about what kind of threshold one is actually estimating. The percentage level of correct answers at which the threshold is estimated lays typically halfway between the guess rate and the 100% level reduced by the lapse rate, i.e., in the 2AFC design of Paper 2 the guess rate was 50% and the lapse rate 5%, therefore, we assessed the 72.5% threshold. 2AFC designs are suitable to estimate grating resolution thresholds, and detection thresholds can be estimated by a 2-interval-forced-choice (2IFC) procedure. In a 2IFC design each trial consists of two time-separated intervals, which are preferably indicated by two different auditory cues. The stimulus is shown in one of the intervals, and the other interval should present a blank screen homogenously set to the average luminance of the stimulus of the other interval.

5.3 Classical psychophysical methods

Once the type of task has been selected, the next design choice concerns the order in which to display the different stimuli strengths. The threshold of the psychometric function can be determined by several psychophysical methods of choosing the next displayed stimulus, but the three **classical psychophysical methods** are: the method of constant stimuli, the method of adjustment, and the method of limits.

In the **method of constant stimuli** a set of stimuli strengths ranging from well below to well above the threshold is predefined. The stimuli are presented to the subject in a randomized order. The randomized stimuli presentation reduces the influence of potential learning effects. The strong advantage of the method of constant stimuli is that it is giving a full description of the psychometric function (it returns both threshold and width of the transition zone) and there is no need of

making initial assumptions about the shape of the function. Therefore the method is sometimes also considered as the gold standard of psychophysics. However, the method of constant stimuli is very time-consuming and therefore risks fatigue of the subject. Furthermore, the high amount of collected data is not used efficiently, which is why it is often not practical to apply this method.

In the **method of adjustment** a range of stimuli strengths is available. The starting point is randomly set, either above or below the threshold, and the subject controls the stimuli strength. It is the subject's assignment to adjust the stimulus strength to its threshold. The procedure is repeated several times and the threshold is estimated by averaging the final stimulus strength of each run. It is a fast procedure and pleasant for the subject. However, since the subject is in control of the stimulus strength and decides the threshold, the method is vulnerable to bias; it is difficult to know what threshold on the psychometric function is used by the individual subjects. To implement the method of adjustment in the Vernier alignment method of Paper 2, the method was further developed: only subjects experienced in psychophysical testing participated in the study. Furthermore, the subjects were instructed to pass the threshold iteratively for a couple of times in both directions to minimize the potential bias.

In the **method of limits** a set of stimuli strengths ranging from well below to well above the threshold is predefined. The stimuli are presented from strongest stimuli strength to weakest, or vice versa. Showing the strongest first will give the subject an impression of what kind of stimulus (s)he is expected to see. The thresholds of an ascending and descending measurement set are often averaged to estimate the threshold. The method of limits is commonly used in the vision clinic to estimate the visual acuity by help of a letter chart. The method of limits is faster than the method of constant stimuli and with a forced-choice design habitational bias (i.e., that the subject continues reporting to see the stimulus even though the threshold was already passed) can be avoided. However, this method is only reporting the threshold but not the width of the transition zone.

5.4 Adaptive psychophysical methods

Adaptive psychophysical methods reduce the data collection need drastically. Whereas in the classical methods the stimulus strengths are entirely set beforehand, the next shown stimulus strength in the adaptive methods depends on the previous response(s) of the subject. Adaptive designs aim to place the next shown stimulus near or at the suspected threshold stimulus strength, thereby avoiding a waste of time far away from the threshold. Different ways of shortening the testing time were put forth by revisions of the method of constant stimuli and the method of limits. As Treutwein pointed out [53], the design choices for these modifications consist of three main criteria: a criterion for how to choose the strength of the next shown stimulus, a stop criterion, and lastly a criterion for what value is taken as the final estimate of the threshold. Depending on the previous knowledge about

the monotony and shape of the psychometric function, either non-parametric or parametric methods can be chosen [53].

Non-parametric methods can estimate the threshold of the psychometric function without any information about its shape, as long as the function is strictly monotonic. A simple example of a non-parameterized method is the truncated staircase, which is a truncated modification of the method of limits. In the truncated staircase, the stimulus strength is altered by a predefined step size after each trial. Moreover, the direction of alteration is reversed when there is a change from responding correctly to incorrectly, or vice versa. In this staircase method the next shown stimulus is only dependent on the just given response. There are many modifications of the staircase method, and an overview can be found in Table 1 of Treutwein's minireview [53]. These modifications vary, among others, in step size (fixed/flexible), their stop criterion (e.g., after how many reversals), and what value is taken as the threshold. In summary, staircase methods are comparably easy to implement, but if the lapse and/or the guess rate is high the threshold estimation is less certain.

For **parametric methods**, one assumes that the psychometric function can be represented by a function with several parameters, where two of them are threshold and slope. In the simplest case the shape of the psychometric function is entirely known and only one parameter is needed, the threshold, which shifts the function along the axis of stimulus strength.

Bayesian methods are a subgroup of parametric adaptive methods. Their strong advantage is the inclusion of all previous responses in the decision about the placement of the next stimulus and the estimation of the final threshold and slope.

The **Ψ-method** by Kontsevich and Tyler is one representative of the Bayesian methods and was applied in Paper 1, 2 and 3 [54]. The psychometric function can be parameterized by a variety of functions, e.g., the Weibull function or the logistic function, which are very similar. In the Ψ-method, we applied the logistic function:

$$\Psi(x) = a + \frac{1 - a - b}{1 + e^{-(x-c)/d}} \tag{5.1}$$

where the stimulus strength x is returning the percentage of correct responses $\Psi(x)$. Furthermore, the function includes the following parameters: the guess rate a, the lapse rate b, the threshold c and the parameter d describing the width of the transition zone. In practice, the guess rate and lapse rate are fixed by the design, but threshold and slope (calculated from the width of the transition zone) are going to be estimated during the experiment.

The Ψ-method can be summarized as follows: The goal is to find the best combination of threshold and slope parameters that describes the psychometric function. Initially, a set of feasible psychometric functions $\Psi_\lambda(x)$ is defined, where each λ describes a certain combination of threshold and slope. Logically, this set also includes the combination with the best description of the relationship between stimulus strengths and corresponding responses. Then, the probability of each combination λ to be the best representation of the true psychometric function, is

measured by the probability distribution $p(\lambda)$. An initial shape of the probability distribution is needed at the start of the procedure and the simplest assumption is an equal probability for all λ. The probability space, formed by the psychometric functions $\Psi_\lambda(x)$ with the corresponding probabilities $p(\lambda)$, can be assessed by its entropy. Smaller entropies relate to growing confidence that the most probable combination λ of threshold and slope represents the true psychometric function. Moreover, the difference in entropy of two succeeding trials corresponds to the gained information. To maximize the gained information in the next trial, the expected entropy for the two possible outcomes (correct/incorrect) for each stimulus strength x is estimated from the previous responses before starting the next trial. The level of the next shown stimulus strength is placed so that it leads to the smallest expected entropy in the upcoming trial and thereby maximizes the gain of information. After the trial, the probability distribution is updated and the entropies are calculated before the subsequent trial. The procedure stops when a predefined number of trials is reached and the combination λ with the highest probability is reported as threshold and slope. The Ψ-method is a good choice to, e.g., measure accurately and efficiently grating acuities at specific contrast levels. Thus, it was used in Paper 1, 2 and 3. However, if the goal is to estimate the full contrast sensitivity function, the Ψ-method would be a very time-consuming measurement procedure.

The **quick CSF method** was developed by Lesmes et al. to quickly estimate the shape of the full CSF [55], and has been implemented for peripheral vision in Paper 1. The main goal here is still to gain the most information with the next shown stimulus. The underlying idea is that the curve of the CSF can be described by a parabolic function with four parameters: peak contrast sensitivity, peak spatial frequency, the bandwidth of the curve and a truncation level at low spatial frequencies. For our peripheral implementation the forth parameter was changed to specify a high-frequency cut-off due to the neural sampling limit. The most likely combination of these four parameters are then found in a procedure similar to the Ψ-method, with the additional complication that there are now two qualities of the stimuli to vary; grating contrast and grating frequency [55]. The method ends after a pre-defined number of trials and reports the most likely combination of the four parameters of the CSF.

5.5 Method implementation and stimuli presentation

Efficient algorithms to measure visual function have been described in the previous section. They can be conveniently implemented in Matlab using the Psychophysics Toolbox extensions [56–58]. However, to successfully quantify properties like contrast sensitivity, resolution acuity or detection acuity, the presentation of a **well-controlled stimulus** to the subject is also required. Since the luminance in cathode ray tubes (CRT) varies non-linearly with the electron-gun voltage, a calibration and subsequent gamma correction of the screen was applied before start

of the psychophysical experiments.

Chapter 4 described the motivation for using gratings as a stimulus choice. To also define at what location in the visual field the test is performed, the gratings need to be spatially confined. This was achieved by the implementation of **Gabor gratings**, which are a product of a sinusoidal grating with a Gaussian envelope (see Fig. 5.2). The advantage of the Gaussian envelope, compared to a circularly truncated grating, is that it gives the stimulus a well-defined spatial location and eliminates sudden luminance changes at the edges of the stimuli. Otherwise, these luminance changes could, for example, bias detection measurements so that the luminance changes at the edges are detected instead of the pattern itself.

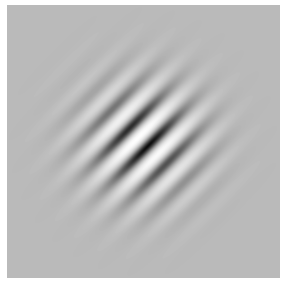

Figure 5.2: Gabor grating. Gabor gratings were implemented as testing stimuli in Paper 1, 2 and 3 to assess detection acuity, resolution acuity and contrast sensitivity. Gabor gratings are a product of a sinusoidal grating with a Gaussian envelope.

Besides a well-defined spatial location of the stimulus, it additionally needs to be ensured that **sufficiently low contrast levels** can be shown to the subject. For example, to have a reasonable approximation of a sinusoidal grating one needs to be able to present at least 4-5 different luminance levels. For a standard computer display the image is presented in 8-bit, or 256 levels of gray. With a minimum of five luminance levels from a dark to a bright fringe and a mean luminance at the center of the full range, the lowest displayable contrast will be $(129-125)/(129+125) = 1.6\%$ corresponding to a maximum CS of 63. Obviously, that is not enough to estimate the full CSF with CS levels up to 100-200, like those needed in Paper 1. Therefore, we implemented the Psychophysics Toolbox extension on a Linux system that allowed a 10-bit stimulus presentation (1024 levels) by direct communication between the extension routines and the drivers of the graphic card. This brings down the lowest displayable contrast to $(514 - 510)/(514 + 510) = 0.4\%$ or a maximum CS of 256, which is more feasible for vision testing.

The psychophysical methods presented in this chapter were applied to compare vision under different magnitudes of TCA: for the contrast sensitity measurements in Paper 1 the Ψ-method and quick CSF method were utilized, visual acuity in Paper 2 and 3 was measured with the Ψ-method in 2AFC/4AFC/2IFC-designs, and the method of adjustment was applied for the Vernier alignment task in Paper 2.

Chapter 6

Measuring Transverse Chromatic Aberration

This chapter presents different techniques used for measuring TCA in the human eye. These techniques are presented in the first two sections and can be categorized into two groups: those that are subjective and those that are objective. In subjective techniques, the subject needs to make a judgment according to a certain criterion. For that reason, subjective methods are limited by the accuracy of the visual system of the subject and vulnerable to decision bias. In contrast, the investigator or an instrument is responsible for the judgment in objective techniques. In this way, the measurement is not depending on the personal interpretation or attention of the subject. Unfortunately, it is not possible to measure TCA with commonly used double pass techniques. However, we present a new method to objectively measure TCA across the visual field of the human eye (see also Paper 5). Additionally, the chapter concludes with some general remarks on the measurement of TCA.

6.1 Subjective measurement techniques

The magnitude of foveal TCA has mainly been assessed by subjective measurement techniques in previous studies as well as in Paper 2. In more recent studies, reported values of foveal TCA have a magnitude up to about 8 arcmin for the spectral range of 430 nm to 770 nm[†] [51,59–62]. But measurement principles as well as the coverage of the visual spectrum vary among studies. Most studies mentioned below, applied different versions of a Vernier alignment task, which had been proposed by Ivanoff, to determine TCA [47].

In the study by Ogboso and Bedell [51], the subject was asked to report alignment of a flashing short wavelength (435 nm) line image relative to a fixed long wave-

[†]Measurement values were recalculated to this range for comparisson, see also Paper 5.

length line image (572 nm). They reported a TCA equivalent to 0.9 to 3.0 arcmin base in (BI)*.

Ogboso and Bedell used natural viewing conditions, whereas in the study by Thibos et al. [59] the subject looked through a displaced pinhole aperture while performing a Vernier alignment task. Thibos et al. recalculated their values to a natural pupil, and reported a magnitude of foveal TCA (433 nm and 622 nm) ranging from 0.36 arcmin BO to 1.67 arcmin BI.

In a third study by Simonet and Campbell [60], two black shadow objects were seen by the subject in a split color field (486 nm and 656 nm) under Maxwellian view†. With the Vernier alignment of the shadow objects they recorded values of 0.25 arcmin BO to 1.56 arcmin BI.

In a fourth study, Rynders et al. [61] applied a two-dimensional, two-color, Vernier alignment target viewed through the natural pupil. The target was presented to the subjects on a standard monitor, and values of TCA were reaching up to 2.5 arcmin.

In contrast to the previously described methods, Marcos et al. [62] utilized a spatially resolved refractometer. In this technique, a test spot is viewed through decentered, changing apertures in the entrance pupil of the eye. The subjects aligned this test spot to a reference target viewed through a central aperture by changing the angle of incidence of the rays from the test spot. Hence, the technique can be described as a subjective polychromatic wavefront sensor that also provides information on the monochromatic errors of the eye. The TCA was estimated with wavelength 473 nm and 601 nm for two subjects showing 2.77 and 3.29 arcmin BI, respectively (the authors reported also what they called pure "optical TCA" as 3.47 and 3.77 arcmin BI).

The magnitude of peripheral TCA has been studied only in very few attempts. Ogboso and Bedell used their technique, previously described for the fovea, also for measurements in the periphery [51]. They measured TCA out to 60° from the fovea and found TCA to increase with eccentricity. The study had a high inter-subject variability with TCA values ranging from 3.9 arcmin BO to 5.3 arcmin BI in the 20° nasal visual field. In Paper 2, the effect of induced TCA on peripheral vision in the 20° nasal visual field was studied. Additionally, a rough estimate of peripheral TCA could be made. The finding of about 1 arcmin BI TCA in the 20° nasal visual field is, however, less than expected by theory (approximately 5 arcmin, Thibos [37]). Both subjective studies showed the need to further improve the methodology to achieve more repeatable estimates of peripheral TCA.

*Base in (BI) and base out (BO) are denoting the orientation of the TCA as applied in this thesis and Paper 2. For example 0.9 arcmin BI means, that this TCA has a magnitude of 0.9 arcmin and a orientation corresponding to TCA caused by a base in aligned prism (base towards the nose) in front of the eye, i.e., short wavelengths will end up at the retina more towards the nasal side than the longer wavelengths.

†Maxwellian view: The light source illuminating the object is imaged to a small point in the eye's pupil [63]. This viewing condition can be used to reduce the influence of monochromatic aberrations on the retinal image quality.

6.2 Objective measurement techniques

The implementation of objective measures of the ocular TCA is challenging, because of the nature of the aberration. All previously described subjective methods are single-pass methods. In single pass methods, the light passes just once through the media of the eye. After the image is formed on the retina, the subject is requested to directly make a subjective judgment according to certain criteria. In contrast, in order to measure any parameter in an objective measurement method, the light also needs to come out of the eye again. So-called double-pass techniques are often applied to obtain objective information on the eye's optical properties and its retinal image quality. However, the asymmetries of odd aberrations, such as coma, distortion and TCA, are canceled out in double pass techniques with the same entrance and exit aperture due to the optical symmetry [64]. In the case of TCA, the single-pass of the chief ray (i.e., a ray entering the eye through the center of the pupil) will result in multiple rays of different wavelength hitting the retina at different positions. In the double-pass regime these rays of different wavelengths will be diffusely reflected and can hence be thought of as multiple sources of different wavelengths at different retinal locations. As the reflected light travels back through the eye, the dispersion will cause the rays of different wavelength to coincide again in the plane of the pupil and leave the eye as one single ray. Therefore, no TCA will be measurable. This cancelling of TCA will also occur in double-pass methods that use entrance and exit apertures of different size, since TCA is independent of pupil size.

However, a new method was developed in Paper 5 to overcome these obstacles of objectively measuring TCA with a double pass technique. In this method, the spatial structure of the retina is recorded in high resolution images with an adaptive optics scanning laser ophthalmoscope (AOSLO). Two wavelengths are used to record the retinal image, and the TCA causes a displacement of the retinal structures between these two images. This displacement is not canceled out when the light is reflected out of the eye again and the method can be seen to correspond to a single-pass methodology. The interleaved recording of the retinal images in two wavelengths therefore allows for a precise measurement of the displacement caused by TCA. An example of a retinal image and more details are given in Fig. 6.1, Paper 5 and by Harmening et al. [65]. Obviously, the measured TCA is a combination of the human eye's TCA and the AOSLO measurement system's TCA. To obtain true measures of the ocular TCA, the AOSLO system's TCA was measured by a specially designed model eye and subtracted from the original measurement data. Paper 5 in this thesis reports the first objective TCA measurements of the central 30° visual field with an average value of 4.0 arcmin in the 10° nasal visual field (543 nm to 842 nm), corresponding to 7.8 arcmin in the spectral range 430 nm to 770 nm. TCA was determined to change with approximately 0.21 arcmin/degree with increasing eccentricity (543 nm to 842 nm, averaged across meridians), which corresponds to a rate of about 0.41 arcmin/degree in the spectral range 430 nm to 770 nm. These measurements are compared to the model eye in Chapter 3 for

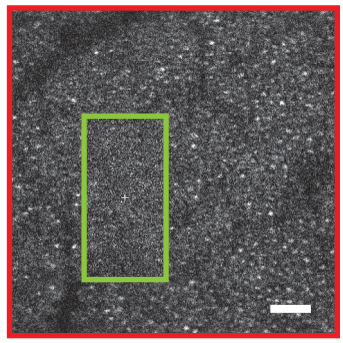

Figure 6.1: Objective TCA measurements with an adaptive optics scanning laser ophthalmoscope (AOSLO). Retinal structures (here shown in the 14° nasal visual field) are recorded interleaved in two wavelengths. The outer red frame marks the retinal area imaged in 842 nm, the inner green frame where the image was recorded interleaved together with the 543 nm channel. The interleaved recording allows for measuring precisely the displacement of the retinal structures, which is caused by TCA. To obtain true measures, the AOSLO system's TCA is measured with a specially designed model eye and subtracted from the human eye's data. Scale bar corresponds to 10 arcmin. Unpublished image from the measurements in Paper 5.

the horizontal visual field in Table 6.1. Here it can be seen, that the angle with no TCA in the measured eyes was located further towards the temporal side than the optical axis in the eye model.

6.3 Remarks on the measurement of TCA

It should be noted that the different techniques described in this chapter include different contributions to the TCA. How subjects experience TCA can depend very much on the specific measurement setup. In some previous subjective studies, e.g., measurements of TCA were divided into optical and perceived TCA [60,62]. In this context, optical TCA means that the light delivery is done via a centered pinhole or Maxwellian view. In contrast, perceived TCA was describing the TCA under more natural viewing conditions like in the study by Ogboso and Bedell [51].

Independent of whether the applied methodology is subjective or objective, there is a need for a few additional considerations for the measurement of TCA as it will depend on several factors. The following paragraphs and related Papers 2, 4 and 5 discuss the effect of the pupil centering, optical correction, and spectrum.

The choice of pupil and its position has a major influence on the measurement of the TCA magnitude. Since any decentration induces additional TCA (as described in Paper 4), the pupil position should be carefully monitored and it should be stated how an artificial pupil is centered. In the natural pupil the centration of the pupil

Table 6.1: Magnitude of measured TCA in the horizontal visual field compared to theory (Paper 5 and eye model in Chapter 3, respectively). TCA magnitude in arcmin, rate in arcmin/degree, spectral range in nm. Sign convention as in Paper 5. *Extrapolation from the foveal data and the rate.

	Paper 5	**Eye Model**		
spectral range	543 - 842	543 - 842	430 - 770	380 - 780
20° nasal	5.9*	5.6	11	16.4
10° nasal	4.0	3.3	6.5	9.7
Fovea	2.1	1.1	2.1	3.2
10° temporal	0.2	-1.1	-2.1	-3.2
20° temporal	-1.7*	-3.3	-6.5	-9.7
rate	0.19	0.23	0.44	0.66

may vary with illumination level [9]. Furthermore, dilation of the pupil has been reported to change position of the pupil center [9, 66, 67]. Consequently, one needs to distinguish between the applications of natural, dilated or artificial pupils.

Monochromatic optical errors can influence the perception of TCA in subjective measurements and reduce the accuracy of objective TCA measurements. If the refractive errors are corrected with trial lenses, any additional TCA from the correction lenses has to be taken into consideration. High-order monochromatic aberrations can be reduced by the use of, e.g., a Maxwellian view [60], a polychromatic wavefront sensor [62], an adaptive optics vision evaluation system (like in Paper 2), or an AOSLO (like in Paper 5).

The magnitude of the TCA will naturally also depend on the spectrum of the light source. Since many different types of spectra are used, there is often a need to recalculate TCA values to compare the results of different studies. Additionally, it is well known that the eye has a varying sensitivity over the spectrum with its peak sensitivity in green under daylight conditions (see Fig. 7.2). In a subjective experiment, it has to be considered whether or not to adjust the luminance of the stimulus for certain wavelengths to balance the neural stimulation over the visual spectrum. While the effect of the eye's spectral sensitivity can be disregarded when discrete wavelengths are used (e.g., laser sources), it should be considered for broad spectrum stimuli where there is a risk of influencing the perception of TCA. Furthermore, in objective techniques different wavelengths may be reflected from different layers in the retina, which would then produce different TCA values compared to what the visual system perceives.

Considering the above mentioned remarks, the objective TCA measurements in Paper 5 took the pupil centration, the correction of monochromatic aberrations, and the difference in reflection into consideration. Furthermore, the technique used two

distinct wavelengths, and the spectrum was recalculated to compare with earlier studies. Hence, the measurements from Paper 5 give an appropriate estimate of TCA across eccentricities.

Chapter 7

Effect of Transverse Chromatic Aberration on Vision

In this chapter, the focus is on the question if and how we can predict the effect of TCA on vision, both for the ocular TCA itself but also induced TCA from optical corrections such as spectacles. This is a question which is dealt with in Paper 2, 3, 4, and 5. In the first section, the contrast reduction and magnification of the retinal image are reviewed. The second section discusses factors that influence perception with TCA. In the third section, the effect of ocular TCA is studied by inducing additional TCA with prisms (spectacles). The forth section compares foveal vision under monochromatic and polychromatic light conditions. Finally, the last section evaluates the effects of ocular TCA on peripheral vision.

7.1 Contrast reduction and image magnification

The retinal image quality plays an important role in the evaluation of vision related to TCA. Here we will look closer at the reduction of contrast and the difference of magnification in the retinal image.

The effect of TCA leads to a reduction of contrast in the retinal image. If one imagines a white light sinusoidal grating as the object, this object can be understood as a superposition of many monochromatic gratings with the same spatial frequency but of different wavelengths. In the formed retinal image, TCA will then shift the gratings of the different wavelengths with respect to each other, and maximum as well as minimum luminance for the different gratings will be on different retinal positions (see Fig. 7.1). The superposition of these single wavelength images will consequently reduce the contrast depending on the spatial frequency. If one assumes a grating consisting of two discrete wavelengths, with a spatial frequency of 7.5 cycles/degree (which is representative for the high contrast visual acuity at 10° eccentricity), and neglect all other aberrations, then already 1 arcmin of TCA would decrease its contrast by approximately 8%. A grating with

a continuous spectrum will be affected by a smaller contrast reduction.

Besides the reduction of contrast, a difference in image magnification can be expected. TCA of extended objects was introduced in Chapter 3 as a difference in magnification for the different wavelengths. This applies to large objects that reach from the fovea out to the periphery. However, it is rare to evaluate vision for such large objects. A typical resolution limit in 10° peripheral visual field is a letter size of 0.25 decimal visual acuity, the whole letter has then a size of 20 arcmin. In Paper 5, TCA was shown to change with a rate of 0.21 arcmin/degree and to reach about 4 arcmin at the same eccentricity. Applying this magnitude of TCA to the described letter size would mean that the change of TCA from the lower edge to the upper edge of the whole letter is only 0.07 arcmin or 0.4% of the whole letter size. This very minimal magnification effect should not be detectable.

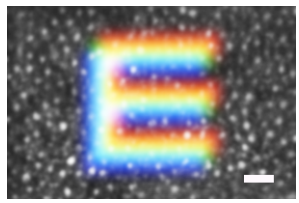

Figure 7.1: Simulation of retinal image quality with TCA in the human eye. The cone mosaic is shown at 10° eccentricity, and the size of letter E corresponds to decimal VA 0.25 (here shown with the letter E, for a grating this would correspond to a spatial frequency of 7.5 cycles/degree). To simulate TCA, the image is composed of three letters E representing blue, green, and red, which are individually blurred by 1 arcmin of gaussian blur (best case scenario for the PSF). The letters are obliquely displaced by 7 arcmin. The scale bar corresponds to 5 arcmin. Unpublished work of Paper 5.

7.2 Factors affecting perception with TCA

The effect of TCA on contrast and image magnification was described in the previous section. However, it is less intuitive to assess how TCA influences vision. When studying vision in relation to TCA we should consider three main parts:

1. the object itself and its spectral characteristics,
2. the path through the dispersive media, and
3. the information processing when the light finally reaches the retina.

In the first part, one can have high impact from TCA (white light) or none at all (monochromatic source) depending on the object's spectrum. TCA also has an asymmetry when it comes to the blurring effect on visual stimuli; the PSF of pure TCA is a line and the blurring is then highly dependent on the orientation of the stimuli. The maximum effect occurs when the blur of TCA is aligned with

the direction of the gratings' modulation. In Paper 2, for example, the contrast reduction of the gratings was only $\frac{1}{\sqrt{2}}$ of the possible maximum, since the gratings were rotated by 45° relative to the TCA blur.

In the second part, TCA originates from the dispersive properties of the media the light travels through, that is the eye together with optical corrections. An increase of the refractive index in, e.g., a spectacle lens will lead to increased dispersion and an increased TCA. Furthermore, a decentered pupil (cf. Paper 4) or a larger visual angle (cf. Paper 5) will also increase the magnitude of TCA. It is worth noting the importance of the direction of TCA: depending on the direction of eccentricity in the visual field the TCA blur will affect different directions of the object, e.g., in the horizontal meridian of the visual field, off-axis TCA will affect mainly vertical lines and correspondingly in other meridians.

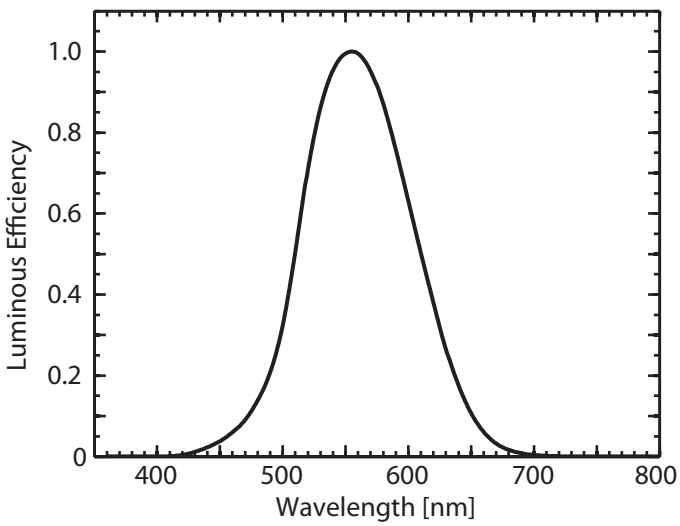

Figure 7.2: Photopic luminous efficiency of the human eye, CIE 1924.

In the third part, the translation of the optical information into neural information in the retina, an important aspect to consider is the luminous efficiency of the eye (see Fig. 7.2). The curve shows that under photopic conditions (luminance above 3 cd/m^2), the eye is most sensitive to light of wavelengths around 555 nm, and the sensitivity becomes significantly lower at the blue or red end of the visual spectrum until it finally reaches zero. This means that the effects of TCA on vision are decreased compared to what could be expected from only considering the retinal image quality. One should note that the presented curve (Fig. 7.2) - which dates back to 1924 - is the currently used standard, but is suspected to underes-

timate luminous efficiency for the shorter wavelengths of the visual spectrum [68]. The neural processing after the optical signal reaches the retina is complex. Cones, responsive to stimuli of different wavelengths, are unevenly distributed over the retina, with the S cones (blue) being sparse over the entire retina and completely absent in the very center of the fovea [69–72]. What kind of color a subject perceives after stimulation of a single cone has been only recently classified; and the response result seems to be dependent on the surrounding cones [73]. Furthermore, neural asymmetries, as described in Paper 3, cause a directional selectivity in the neural processing of objects. It was shown in Paper 3 that the gain in visual acuity by changing from perpendicular gratings to parallel gratings for polychromatic stimuli is the largest in the nasal visual field. As shown in Paper 5, the nasal visual field is also where the ocular TCA is largest. Additionally, the polychromatic peripheral contrast sensitivity is significantly different between different visual field directions, i.e., the horizontal and the vertical meridian, which was shown in Paper 1.

7.3 Visual effect of changing the magnitude of TCA

One opportunity to access the impact of TCA on vision is to increase or decrease the magnitude of TCA in the retinal image, without changing the spectrum of the object. This can be achieved with the help of prisms, since any polychromatic light beam going through a thin prism will undergo dispersion and show almost pure TCA effects when exiting the prism again (see Fig. 7.3). Given the deviation angle of the prism, ν, and the Abbe number, V, the induced TCA is approximately $\frac{\nu}{V}$. By placing a prism in front of the eye, the additional TCA in the prism can either add to the existing ocular TCA, and thereby increase the total magnitude of TCA in the retinal image, or cancel the ocular TCA, partly or completely. This was the method implemented in Paper 2.

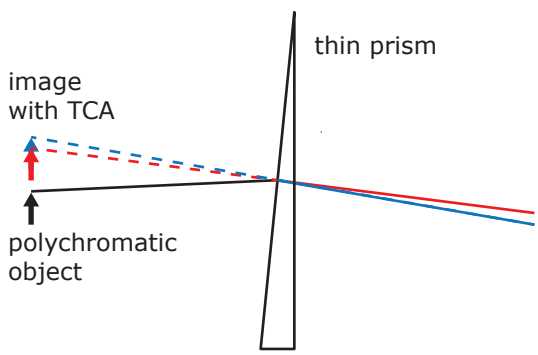

Figure 7.3: Schematic illustration showing how dispersion in a thin prism leads to pure TCA of an image. The same principle was utilized in Paper 2 to induce TCA.

In the fovea, earlier studies used contrast sensitivity measurements to show that the contrast is reduced due to induced TCA [74–77]. Furthermore, it was shown that the visual acuity is also reduced [78,79]. For the quantification of the effects of induced TCA by spectacles or prisms, it is important to access carefully how much TCA is actually induced. As shown in Paper 2, the simple report of prismatic power and Abbe number can overestimate the magnitude of induced TCA and therefore underestimate the effect of TCA on vision. Recalculating the results, given by Meslin [78] and Kampmeier [79], only with the Abbe number estimates the influence of TCA on foveal resolution acuity to be 0.01 - 0.02 logMAR/arcmin. However, an effect of 0.03 logMAR/arcmin of induced TCA on foveal grating resolution was shown in Paper 2.

In the periphery, the effect of induced TCA increases: we showed that grating detection acuity in the 20° nasal field worsens by more than 0.05 logMAR/arcmin. We suggested that this difference over the visual field can be understood through the difference in shape between the peripheral detection contrast sensitivity function (CSF) and the foveal resolution contrast sensitivity function. As grating acuity corresponds to the high frequency cutoff of the CSF, its reduction with contrast degradation is dependent on the slope of the CSF near the high frequency cutoff. A reduction in the overall contrast of the retinal image by induced TCA can be imagined as a downwards shift of the CSF, whereby changing its cutoff frequency; with a flatter curve resulting in a larger alteration of the cutoff frequency. As can be seen in Fig. 4.4 in Chapter 4, the peripheral detection CSF with its aliased parts becomes flatter than the foveal CSF, which explains the larger effect of induced TCA on peripheral detection compared to foveal resolution acuity. In this context, it should be remembered that this flattening of the peripheral detection CSF due to aliasing is already apparent with spectacles for correcting the peripheral refractive errors and does not necessitate adaptive optics correction [46]. Consequently, it was concluded in Paper 2, that the success of spectacles optimized for peripheral vision is dependent on including appropriate choices of the parameters related to TCA (e.g., prism reference point, the prismatic power, and the applied lens material) in the spectacle design process.

7.4 Foveal vision in monochromatic and polychromatic light

Another way to evaluate the effect of TCA on vision is by changing the spectrum of the object from white light to monochromatic conditions (see, for example, Campbell and Gubisch [80], Yoon and Williams [81], and Schwarz et al. [82]). Naturally, this spectral narrowing will reduce both of the chromatic aberrations, TCA and LCA, but may also decrease luminance and color information. In 1967, Campbell and Gubisch [80] recognized an improvement of only 6% in foveal visual acuity (from 52 to 55 cycles/degree, 2.5 mm artificial pupil aperture) when changing from a white light source to a yellow filter (578 nm). On the other hand, foveal contrast sensitivity at 30 cycles/degree increased by about 31% under natural accommoda-

tion, and 55% under paralyzed accommodation, for a 2.5 mm pupil. However, when increasing pupil size to 4 mm, Campbell and Gubisch reported a diminished effect and speculated about spherical aberration being the cause. Almost 50 years later, Schwarz et al. [82] compared binocular decimal visual acuity for a 4.8 mm artificial pupil in polychromatic light (LED microdisplay) with monochromatic conditions (550 nm filter). They measured an average improvement in binocular decimal visual acuity of about 34% (0.80 to 1.07) with spherical aberration present, and a similar improvement of 29% (0.93 to 1.20) when spherical aberration was corrected. In conclusion, both studies consistently indicate that changing from polychromatic to monochromatic conditions improves visual acuity.

7.5 Evaluating the effects of ocular TCA on peripheral vision

For peripheral vision, the effect of monochromatic stimuli compared to white light stimuli is less known. This question was addressed by Paper 3, where the peripheral detection acuity for both polychromatic and monochromatic stimuli was evaluated, and it was studied if there is any preference for different stimulus orientations. It was shown that the visibility of a grating depends on its orientation relative to the visual field meridian tested (for orientations see Fig. 7.4). Because peripheral TCA generates blur mainly in the radial direction, one would expect that TCA has a larger influence on gratings perpendicular to the field meridian than on parallel gratings (for which TCA should have a minimum effect). In the experiments of Paper 3, the detection acuity for polychromatic stimuli of subject 1 was 0.72 logMAR for the perpendicular and 0.43 logMAR for the parallel gratings in the 20° nasal visual field. Going from polychromatic to monochromatic stimuli (543 nm filter) the acuity for the perpendicular grating should have improved, since we reduced the blurring effect of TCA. However, the luminances of the stimuli for the monochromatic and polychromatic cases were not matched, and the luminance was lower in the monochromatic case due to the filter. It is well known that visual acuity depends on illumination [83]. Therefore, the measured acuity for monochromatic stimuli was 0.74 logMAR for the perpendicular and 0.64 logMAR for the parallel gratings.

Despite the difference in luminance, the results of Paper 3 clearly show that the visual acuity for the monochromatic condition worsened much more for parallel gratings (minimal influence of TCA, from 0.43 logMAR to 0.64 logMAR) than for perpendicular gratings (from 0.72 logMAR to 0.74 logMAR). These numbers contain a worsening due to the decreased luminance (that may be assumed to be similar for both orientations), an improvement due to minimizing LCA (also assumed to be similar for both orientations), but also an improvement due to minimizing TCA. With this argumentation, the 0.19 logMAR difference in acuity degradation between the two grating orientations can be seen as a consequence of the reduced blurring by TCA. In a similar study by Cheney et al. the effect of TCA on periph-

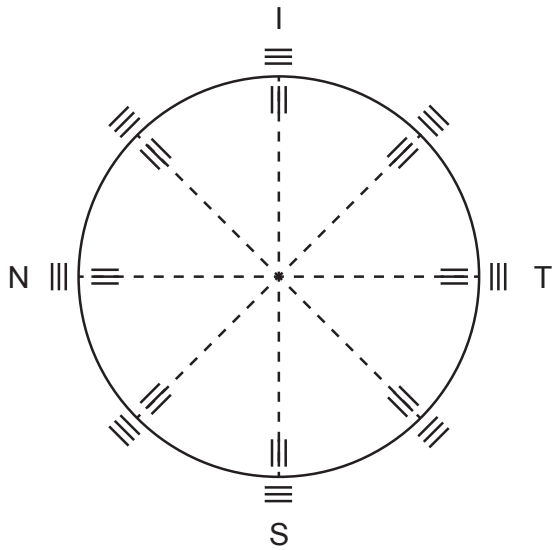

Figure 7.4: Schematic representation of the different visual field meridians for the right eye used in Paper 3: temporal (T), superior (S), nasal (N), and inferior (I). The solid circle represents the 20° eccentricity and the center of the circle denotes the central visual field. The lines inside the circle represent parallel, and the lines outside the circle represent perpendicular grating orientations. Adapted from Paper 3.

eral detection of perpendicular gratings was also found to be larger than the effect on parallel gratings [84]. It can be speculated that this difference of 0.19 logMAR might be considered as a first estimate of the influence of the ocular TCA on peripheral detection acuity under adaptive optics correction in the 20° nasal visual field.

The gain in acuity by correcting TCA was also measured with a different method in Paper 2 for the same subject and the same visual field as in Paper 3: the detection acuity for obliquely oriented gratings improved by 0.10 logMAR when the ocular TCA was corrected with a BO-prism (measured acuity for subject 1 in Paper 2 and 3). Correcting this number by a factor of $\sqrt{2}$ for the oblique stimuli orientation gives a difference of 0.14 logMAR between with and without TCA. Considering that LCA remained uncorrected in Paper 2, it seems reasonable that this acuity improvement of 0.14 logMAR is slightly lower than the 0.19 logMAR derived from Paper 3.

To summarize, TCA is causing a contrast reduction that depends on the orientation of the object, and this contrast reduction then affects peripheral detection acuity and contrast sensitivity. Since peripheral resolution acuity is sampling limited, it is not affected by the contrast reduction caused by TCA.

Chapter 8

Conclusions and Outlook

This thesis is about transverse chromatic aberration and vision. Summarizing the results, this work has concentrated on developing methodology to objectively measure TCA across the visual field and to evaluate peripheral vision. Furthermore, we have presented results important for low vision rehabilitation as well as for retinal imaging applications.

We demonstrated how to objectively measure TCA over an extended visual field and found TCA to increase linearly with eccentricity; about 0.21 arcmin per degree for the spectral range 543 nm to 842 nm (Paper 5). Furthermore, we measured the peripheral TCA to be approximately 4.0 arcmin in the 10° nasal visual field. These measurements were performed with an adaptive optics scanning laser ophthalmoscope (AOSLO) and utilized a specially designed physical eye model to measure and correct for the AOSLO system's own TCA. We demonstrated that pupil tracking can be used to estimate relative changes in TCA caused by small shifts in the pupil alignment, and showed that the compensation for these shifts improves the measurement of TCA as a function of eccentricity (Paper 4).

To evaluate vision, we implemented a quick adaptive Bayesian routine to measure the complete contrast sensitivity function in the peripheral human eye (Paper 1). In this routine we utilize gratings as visual stimuli that are oriented obliquely relative to the visual field meridian. We also showed that these grating orientations are suitable for the evaluation of peripheral vision (Paper 3). Moreover, we investigated the effect of prism-induced TCA on vision under adaptive optics correction in the central and peripheral visual field, and found the influence of TCA to be higher on peripheral grating detection than on foveal grating resolution (Paper 2). Peripheral grating detection acuity was shown to degrade by more than 0.05 logMAR per arcmin of induced TCA, whereas foveal resolution degraded by about 0.03 logMAR/arcmin.

The results of this thesis have several applications in clinical practice, fundamental research and instrumentation development motivating further investigation:

1. When the peripheral refractive errors of the eye are to be corrected, e.g., for people suffering from macular degeneration and central visual field loss, any additional peripheral TCA will reduce their remaining vision. Even though an adaptive optics system was utilized in this work, full correction of high-order monochromatic aberrations is probably not required to notice the effects of TCA on peripheral vision. In the future, it is interesting to study how peripheral optical corrections can be designed to also compensate for TCA.

2. For understanding the process of myopia development and the growth of the eye, the magnitude of TCA across the visual field should be also measured in myopic eyes. Potential differences in the magnitude of TCA between myopic and emmetropic eyes could indicate that TCA is involved in the regulating processes of eye growth.

3. In applications of retinal imaging, TCA leads to lateral offsets when utilizing more than one wavelength. The measurement of TCA together with careful pupil alignment and subsequent compensation can improve the functionality of these systems.

Bibliography

[1] J. Gustafsson and P. Unsbo, "Eccentric correction for off-axis vision in central visual field loss.", *Optometry and Vision Science* **80**, 535 (2003).

[2] L. Lundström, J. Gustafsson, and P. Unsbo, "Vision evaluation of eccentric refractive correction.", *Optometry and Vision Science* **84**, 1046 (2007).

[3] K. Baskaran, R. Rosén, P. Lewis, P. Unsbo, and J. Gustafsson, "Benefit of Adaptive Optics Aberration Correction at Preferred Retinal Locus", *Optometry and Vision Science* **89**, 1417 (2012).

[4] B. Holden, P. Sankaridurg, E. Smith, T. Aller, M. Jong, and M. He, "Myopia, an underrated global challenge to vision: where the current data takes us on myopia control.", *Eye* **28**, 142 (2014).

[5] A. Roorda, F. Romero-Borja, W. Donnelly, H. Queener, T. Hebert, and M. Campbell, "Adaptive optics scanning laser ophthalmoscopy.", *Optics Express* **10**, 405 (2002).

[6] R. B. Rabbetts, *Bennett and Rabbett's Clinical Visual Optics*, Butterworth-Heinemann, Philadelphia, 4th edition (2007).

[7] D. A. Atchison and G. Smith, *Optics of the Human Eye*, Butterworth-Heinemann, Edinburgh (2000).

[8] M. Millodot, *Dictionary of Optometry and Visual Science*, Butterworth-Heinemann, Oxford, 4th edition (1997).

[9] M. A. Wilson, M. C. W. Campbell, and P. Simonet, "The Julius F. Neumueller Award in Optics, 1989: Change of Pupil Centration with Change of Illumination and Pupil Size", *Optometry and Vision Science* **69**, 129 (1992).

[10] E. Donnenfeld, "The Pupil is a Moving Target: Centration, Repeatability, and Registration", *Journal of Refractive Surgery* **20**, S593 (2004).

[11] P. Lewis, *Improving peripheral vision through optical correction and stimulus motion*, Ph.D. thesis, Linnaeus University Kalmar (2016).

[12] D. Malacara-Hernandez, M. Carpio-Valadez, and J. J. Sanchez-Mondragon, "Wavefront fitting with discrete orthogonal polynomials in a unit radius circle", *Optical Engineering* **29**, 672 (1990).

[13] International Organization for Standardization, "Ophthalmic optics and instruments - Reporting aberrations of the human eye", *ISO 24157:2008(en)* (2008).

[14] American National Standards Institute, "Methods for reporting optical aberrations of eyes", *ANSI Z80.28-2004* (2004).

[15] L. Lundström, *Wavefront aberrations and peripheral vision*, Ph.D. thesis, KTH Royal Institute of Technology (2007).

[16] Rocchini, "The Zernike polynomials values, https://commons.wikimedia.org/wiki/File: Zernike_polynomials2.png, accessed 2016-04-07", (2008).

[17] J. Liang, D. R. Williams, and D. T. Miller, "Supernormal vision and high-resolution retinal imaging through adaptive optics.", *Journal of the Optical Society of America A* **14**, 2884 (1997).

[18] J. Gustafsson, E. Terenius, J. Buchheister, and P. Unsbo, "Peripheral astigmatism in emmetropic eyes", *Ophthalmic and Physiological Optics* **21**, 393 (2001).

[19] L. Lundström, J. Gustafsson, and P. Unsbo, "Population distribution of wavefront aberrations in the peripheral human eye.", *Journal of the Optical Society of America A* **26**, 2192 (2009).

[20] P. Lewis, K. Baskaran, R. Rosén, L. Lundström, P. Unsbo, and J. Gustafsson, "Objectively determined refraction improves peripheral vision.", *Optometry and Vision Science* **91**, 740 (2014).

[21] A. Seidemann, F. Schaeffel, A. Guirao, N. Lopez-Gil, and P. Artal, "Peripheral refractive errors in myopic, emmetropic, and hyperopic young subjects.", *Journal of the Optical Society of America A* **19**, 2363 (2002).

[22] R. Navarro, E. Moreno, and C. Dorronsoro, "Monochromatic aberrations and point-spread functions of the human eye across the visual field.", *Journal of the Optical Society of America A* **15**, 2522 (1998).

[23] D. A. Atchison and D. H. Scott, "Monochromatic aberrations of human eyes in the horizontal visual field.", *Journal of the Optical Society of America A* **19**, 2180 (2002).

[24] J. Porter, A. Guirao, I. G. Cox, and D. R. Williams, "Monochromatic aberrations of the human eye in a large population", *Journal of the Optical Society of America A* **18**, 1793 (2001).

[25] F. W. Campbell, J. J. Kulikowski, and J. Levinson, "The effect of orientation on the visual resolution of gratings", *The Journal of Physiology* **187**, 427 (1966).

[26] J. Rovamo, V. Virsu, P. Laurinen, and L. Hyvärinen, "Resolution of gratings oriented along and across meridians in peripheral vision.", *Investigative Ophthalmology & Visual Science* **23**, 666 (1982).

[27] W. Geisler and M. Banks, "Visual performance", in M. Bass (editor), "Handbook of optics I", chapter 25, pages 25.1–25.55, McGraw-Hill, New York, 2nd edition (1995).

[28] C. A. Curcio, K. R. Sloan, R. E. Kalina, and a. E. Hendrickson, "Human photoreceptor topography.", *The Journal of Comparative Neurology* **292**, 497 (1990).

[29] C. A. Curcio and K. A. Allen, "Topography of ganglion cells in human retina.", *The Journal of Comparative Neurologyeurology* **300**, 5 (1990).

[30] Y. Le Grand, *Optique physiologique. Tome troisième, L'espace visuel*, Revue d'optique, Paris (1956).

[31] J. G. Sivak and T. Mandelman, "Chromatic dispersion of the ocular media.", *Vision Research* **22**, 997 (1982).

[32] M. C. Rynders, R. Navarro, and M. A. Losada, "Objective measurement of the off-axis longitudinal chromatic aberration in the human eye", *Vision Research* **38**, 1 (1998).

[33] B. Jaeken, L. Lundström, and P. Artal, "Peripheral aberrations in the human eye for different wavelengths: off-axis chromatic aberration", *Journal of the Optical Society of America A* **28**, 1871 (2011).

[34] A. Cornu, "Sur le spectre normal du Soleil, Partie ultra-violette", *Annales scientifiques de l'École Normale Supérieure 2e serie* **9**, 21 (1880).

[35] J. Hartmann, "Über eine einfache Interpolationsformel für das prismatische Spektrum", *Publikationen des Astrophysikalischen Observatoriums zu Potsdam* **12**, Anhang 1 (1898).

[36] D. A. Atchison and G. Smith, "Chromatic dispersions of the ocular media of human eyes.", *Journal of the Optical Society of America A* **22**, 29 (2005).

[37] L. Thibos, "Calculation of the influence of lateral chromatic aberration on image quality across the visual field", *Journal of the Optical Society of America A* **4**, 1673 (1987).

[38] L. Thibos, M. Ye, X. Zhang, and A. Bradley, "The chromatic eye: a new reduced-eye model of ocular chromatic aberration in humans", *Applied Optics* pages 3594–3600 (1992).

[39] L. N. Thibos, M. Ye, X. X. Zhang, and A. Bradley, "Spherical aberration of the reduced schematic eye with elliptical refracting surface", *Optometry and Vision Science* **74**, 548 (1997).

[40] J. W. Goodman, *Introduction to Fourier Optics*, McGraw-Hill, Singapore, 2nd edition (1996).

[41] R. L. De Valois and K. K. De Valois, *Spatial Vision*, Oxford University Press, New York (1990).

[42] L. N. Thibos, F. E. Cheney, and D. J. Walsh, "Retinal limits to the detection and resolution of gratings.", *Journal of the Optical Society of America A* **4**, 1524 (1987).

[43] L. Lundström, S. Manzanera, P. M. Prieto, D. B. Ayala, N. Gorceix, J. Gustafsson, P. Unsbo, and P. Artal, "Effect of optical correction and remaining aberrations on peripheral resolution acuity in the human eye", *Optics Express* **15**, 12654 (2007).

[44] H. Nyquist, "Certain Topics in Telegraph Transmission Theory", *Transactions of the American Institute of Electrical Engineers* **47**, 617 (1928).

[45] L. N. Thibos, D. J. Walsh, and F. E. Cheney, "Vision beyond the resolution limit: Aliasing in the periphery", *Vision Research* **27**, 2193 (1987).

[46] L. N. Thibos, D. L. Still, and A. Bradley, "Characterization of spatial aliasing and contrast sensitivity in peripheral vision.", *Vision Research* **36**, 249 (1996).

[47] A. Ivanoff, "Sur une méthode de mesure des aberrations chromatiques et sphériques de l'oeil en luminière dirigée", in "Comptes Rendus Hebdomadaires des Séances de l'Académie des Sciences", volume 223, pages 170 –172, Gauthier-Villars, Paris (1946).

[48] B. Bourdon, *La perception visuelle de l'espace*, Schleicher Frères, Paris (1902).

[49] G. Westheimer, "The spatial grain of the perifoveal visual field", *Vision Research* **22**, 157 (1982).

[50] D. M. Levi, S. A. Klein, and A. P. Aitsebaomo, "Vernier acuity, crowding and cortical magnification", *Vision Research* **25**, 963 (1985).

[51] Y. U. Ogboso and H. E. Bedell, "Magnitude of lateral chromatic aberration across the retina of the human eye", *Journal of the Optical Society of America A* **4**, 1666 (1987).

[52] T. T. Norton, D. A. Corliss, and J. E. Bailey, *The Psychophysical Measurement of Visual Function*, Richmond Products, Albuquerque (2002).

[53] B. Treutwein, "Adaptive Psychophysical Procedures", *Vision Research* **35**, 2503 (1995).

[54] L. L. Kontsevich and C. W. Tyler, "Bayesian adaptive estimation of psychometric slope and threshold.", *Vision Research* **39**, 2729 (1999).

[55] L. A. Lesmes, Z.-L. Lu, J. Baek, and T. D. Albright, "Bayesian adaptive estimation of the contrast sensitivity function: The quick CSF method", *Journal of Vision* **10**, 17 (2010).

[56] D. H. Brainard, "The Psychophysics Toolbox.", *Spatial Vision* **10**, 433 (1997).

[57] D. G. Pelli, "The VideoToolbox software for visual psychophysics: transforming numbers into movies.", *Spatial Vision* **10**, 437 (1997).

[58] M. Kleiner, D. H. Brainard, D. G. Pelli, C. Broussard, T. Wolf, and D. Niehorster, "What's new in Psychtoolbox-3?", *Perception* **36**, S14 (2007).

[59] L. N. Thibos, A. Bradley, D. L. Still, X. Zhang, and P. A. Howarth, "Theory and measurement of ocular chromatic aberration", *Vision Research* **30**, 33 (1990).

[60] P. Simonet and M. C. Campbell, "The optical transverse chromatic aberration on the fovea of the human eye.", *Vision Research* **30**, 187 (1990).

[61] M. Rynders, B. Lidkea, W. Chisholm, and L. N. Thibos, "Statistical distribution of foveal transverse chromatic aberration, pupil centration, and angle psi in a population of young adult eyes.", *Journal of the Optical Society of America A* **12**, 2348 (1995).

[62] S. Marcos, S. A. Burns, E. Moreno-Barriusop, and R. Navarro, "A new approach to the study of ocular chromatic aberrations.", *Vision Research* **39**, 4309 (1999).

[63] G. Westheimer, "The Maxwellian view.", *Vision Research* **6**, 669 (1966).

[64] P. Artal, S. Marcos, R. Navarro, and D. R. Williams, "Odd aberrations and double-pass measurements of retinal image quality", *Journal of the Optical Society of America A* **12**, 195 (1995).

[65] W. M. Harmening, P. Tiruveedhula, A. Roorda, and L. C. Sincich, "Measurement and correction of transverse chromatic offsets for multi-wavelength retinal microscopy in the living eye", *Biomedical Optics Express* **3**, 2066 (2012).

[66] G. Walsh, "The effect of mydriasis on the pupillary centration of the human eye.", *Ophthalmic and Physiological Optics* **8**, 178 (1988).

[67] T. A. Hoang, J. E. Macdonnell, M. C. Mangan, C. S. Monsour, B. L. Polwattage, S. F. Wilson, M. Suheimat, and D. A. Atchison, "Time Course of Pupil Center Location After Ocular Drug Application.", *Optometry and Vision Science* **93** (2016).

[68] E. F. Schubert, "Human eye sensitivity and photometric quantities", in "Light-Emitting Diodes", chapter 16, Cambridge University Press, New York, 2nd edition (2006).

[69] C. A. Curcio, K. A. Allen, K. R. Sloan, C. L. Lerea, J. B. Hurley, I. B. Klock, and A. H. Milam, "Distribution and morphology of human cone photoreceptors stained with anti-blue opsin", *Journal of Comparative Neurology* **312**, 610 (1991).

[70] A. Roorda and D. R. Williams, "The arrangement of the three cone classes in the living human eye", *Nature* **397**, 520 (1999).

[71] H. Hofer, J. Carroll, J. Neitz, M. Neitz, and D. R. Williams, "Organization of the human trichromatic cone mosaic.", *The Journal of Neuroscience* **25**, 9669 (2005).

[72] R. Sabesan, H. Hofer, and A. Roorda, "Characterizing the Human Cone Photoreceptor Mosaic via Dynamic Photopigment Densitometry", *PLoS ONE* **10**, 1 (2015).

[73] R. Sabesan, B. Schmidt, W. S. Tuten, A. Boehm, and A. Roorda, "Functional organization of color in the trichromatic cone mosaic", *Investigative Ophthalmology & Visual Science* **56**, 4013 (2015).

[74] A. El-Kadouri and W. N. Charman, "Chromatic aberration in prismatic corrections", in "Transactions of the First International Congress, The Frontiers of Optometry (British College of Ophthalmic Opticians, 1984)", volume 2, pages 154–160 (1984).

[75] C. Y. Tang and W. N. Charman, "Effects of monochromatic and chromatic oblique aberrations on visual performance during spectacle lens wear.", *Ophthalmic and Physiological Optics* **12**, 340 (1992).

[76] C. M. Fonseka and H. Obstfeld, "Effect of the constringence of afocal prismatic lenses on monocular acuity and contrast sensitivity.", *Ophthalmic and Physiological Optics* **15**, 73 (1995).

[77] J. Faubert, P. Simonet, and J. Gresset, "Effects of induced transverse chromatic aberration from an afocal prismatic lens on spatio-temporal sensitivity", *Ophthalmic and Physiological Optics* **19**, 336 (1999).

[78] D. Meslin and G. Obrecht, "Effect of chromatic dispersion of a lens on visual acuity.", *American Journal of Optometry and Physiological Optics* **65**, 25 (1988).

[79] E. Kampmeier, "Die neue Airwear-Brillenglasgeneration - Einfluss der chromatischen Aberration auf die Sehschärfe", *Optometrie* **1**, 10 (1999).

[80] F. W. Campbell and R. W. Gubisch, "The effect of chromatic aberration on visual acuity.", *The Journal of Physiology* **192**, 345 (1967).

[81] G.-Y. Yoon and D. R. Williams, "Visual performance after correcting the monochromatic and chromatic aberrations of the eye", *Journal of the Optical Society of America A* **19**, 266 (2002).

[82] C. Schwarz, C. Cánovas, S. Manzanera, H. Weeber, P. M. Prieto, P. Piers, and P. Artal, "Binocular visual acuity for the correction of spherical aberration in polychromatic and monochromatic light.", *Journal of Vision* **14** (2014).

[83] S. Shlaer, "The relation between visual acuity and illumination", *The Journal of General Physiology* **21**, 165 (1937).

[84] F. Cheney, L. Thibos, and A. Bradley, "Effect of ocular transverse chromatic aberration on detection acuity for peripheral vision", *Ophthalmic and Physiological Optics* **35**, 70 (2015).

Acknowledgements

I am very grateful for the support of many people who first made writing this thesis possible. I wish to express my warmhearted gratitude to all of you, even though you might not be mentioned explicitly below.

Particularly, I would like to thank my fantastic supervisors Linda Lundström, Peter Unsbo, and Hans Hertz: Thank you for your encouraging guidance and leadership through the years of ups and downs of my Phd student life.

I am also very grateful to my Phd student "siblings": Abinaya Venkataraman and Robert Rosén, it is great that we have met. Thank you for all words of wisdom and laughter you have shared with me.

Furthermore, I am grateful to my present and past colleagues at BioX: Thank you for making our corridor to such a pleasant and unique place to work at. Additionally, I have received valuable support from our workshop at KTH, the administration and many more persons.

During the past years at KTH, I have had the privilege to collaborate with inspiring people around the world. In particular, I wish to express my gratitude to my colleagues at the Rodenstock GmbH (Munich, Germany) and the Roorda laboratory at the University of California (Berkeley, California, USA) for the exciting projects and lively discussions we have had together. Moreover, I have had the pleasure to meet and discuss with researchers at Karolinska Institutet (Stockholm, Sweden), St. Erik's eye hospital (Stockholm, Sweden), the University of Kalmar (Kalmar, Sweden), University College of Southeast Norway (Kongsberg, Norway), University of Tuebingen (Tuebingen, Germany), CSIC (Madrid, Spain), Laboratorio de Optica (Murcia, Spain), the University of Crete (Heraklion, Greece), and at several conferences. Thank you for your inspiration.

Last but not least I want to thank my family and my friends: It is you who gave me the energy to pursue this project and I feel very gifted to have you all in my life. Thank you for being how you are.

Summary of the Original Work

This thesis is based on the following five papers investigating the impact of chromatic errors across the visual field of the human eye. The focus lays on the transverse chromatic aberration (TCA). The author has been the main responsible for Paper 2 and 5, including study design, execution of experiments, analysis of results and writing the papers. The author was main responsible for design and implementation of the stimulus presentation system used for the measurements in Paper 1, 2 and 3. In Paper 1 and 3, the author was jointly responsible for study design and execution of measurements, and contributed to data analysis and the writing of the manuscript. In Paper 4, the author led the planning, implementation and execution of the TCA measurements over the visual field, jointly conceived the original idea, and contributed to the writing of the manuscript. For Paper 4 and 5, the author initiated a new collaboration with the Roorda laboratory at the University of California, Berkeley, and the experiments utilized their adaptive optics scanning laser ophthalmoscope. The study in Paper 2 was performed in collaboration with the Rodenstock GmbH in Munich.

Paper 1 **Quick contrast sensitivity measurements in the periphery**

This paper presents the implementation and evaluation of a quick routine to measure the complete contrast sensitivity function in the peripheral human eye. Furthermore, the polychromatic peripheral contrast sensitivity was shown to be significantly different between the horizontal and the vertical meridian.

Paper 2 **Effect of induced transverse chromatic aberration on peripheral vision**

In this paper, the effect of prism-induced horizontal TCA on vision, in the central as well as in the 20° nasal visual field is investigated. The influence of TCA on peripheral grating detection was found to be higher than on foveal grating resolution. Furthermore, the study concludes that inducing additional peripheral TCA should be avoided when the peripheral refractive errors of the eye are to be corrected.

Paper 3 **Choice of grating orientation for evaluation of peripheral vision**

This paper evaluates the importance of choosing the appropriate grating orientation for the evaluation of peripheral vision. To reduce measurement variation, it is recommend to use gratings, which are obliquely oriented relative to the visual field meridian, as stimuli. The paper discusses the meridional effect for both polychromatic and monochromatic stimuli and thereby rules out the presence of the meridional effect only due to TCA.

Paper 4 **Eye-tracking technology for real-time monitoring of transverse chromatic aberration**

This paper demonstrates that pupil tracking can measure relative changes in TCA caused by small shifts in the pupil alignment of an adaptive optics scanning laser ophthalmoscope (AOSLO). The compensation for these shifts improves the measurement of TCA as a function of eccentricity. Consequently, the functionality of AOSLO systems can be improved by the control of TCA.

Paper 5 **Transverse chromatic aberration across the visual field of the human eye**

This paper presents the first objective technique to estimate the ocular TCA over the human visual field. With the combination of the spatial structure of high-resolution retinal images and a physical eye model without TCA, it is possible to overcome the difficulties in objectively measuring TCA with existing techniques. The results of the paper show a linear increase of TCA with off-axis field angle.